7-1-2010

Apo B100 similarities to viral proteins suggest basis for LDL-DNA binding and transfection capacity

Juan Guevara

Nagindra Prashad

Boris Ermolinsky

John W. Gaubatz

Dongcheul Kang

See next page for additional authors

Recommended Citation

Juan Guevara, et. al., (2010) Apo B100 similarities to viral proteins suggest basis for LDL-DNA binding and transfection capacity.Journal of Lipid Research51:71704. DOI: http://doi.org/10.1194/jlr.M003277

Apo B100 similarities to viral proteins suggest basis for LDL-DNA binding and transfection capacity

Juan Guevara, Jr., Nagindra Prashad,[2] Boris Ermolinsky,[3] John W. Gaubatz,[4] Dongcheul Kang,[5] Andrea E. Schwarzbach,[6] David S. Loose,[7] and Natalia Valentinova Guevara[1]

Department of Physics and Astronomy, University of Texas Brownsville/Texas Southmost College, Brownsville, TX 78520

Abstract **LDL mediates transfection with plasmid DNA in a variety of cell types in vitro and in several tissues in vivo in the rat. The transfection capacity of LDL is based on apo B100, as arginine/lysine clusters, suggestive of nucleic acid-binding domains and nuclear localization signal sequences, are present throughout the molecule. Apo E may also contribute to this capacity because of its similarity to the Dengue virus capsid proteins and its ability to bind DNA. Synthetic peptides representing two apo B100 regions with prominent Arg/Lys clusters were shown to bind DNA. Region 1 (^{0014}Lys-Ser^{0160}) shares sequence motifs present in DNA binding domains of Interferon Regulatory Factors and *Flaviviridae* capsid/core proteins. It also contains a close analog of the B/E receptor ligand of apo E. Region 1 peptides, B1-1 (^{0014}Lys-Glu^{0054}) and B1-2 (^{0055}Leu-Ala^{0096}), mediate transfection of HeLa cells but are cytotoxic. Region 2 (^{3313}Asp-Thr^{3431}), containing the known B/E receptor ligand, shares analog motifs with the human herpesvirus 5 immediate-early transcriptional regulator (UL122) and *Flaviviridae* NS3 helicases. Region 2 peptides, B2-1 (^{3313}Asp-Glu^{3355}), and B2-2 (^{3356}Gly-Thr^{3431}) are ineffective in cell transfection and are noncytotoxic. These results confirm the role of LDL as a natural transfection vector in vivo, a capacity imparted by the apo B100, and suggest a basis for *Flaviviridae* cell entry.**—Guevara, J., Jr., N. Prashad, B. Ermolinksy, J. W. Gaubatz, D. Kang, A. E. Schwarzbach, D. S. Loose, and N. V. Guevara. **Apo B100 similarities to viral proteins suggest basis for LDL-DNA binding and transfection capacity. *J. Lipid Res.* 2010.** 51: **1704–1718.**

Supplementary key words *Flaviviridae* capsid/core proteins • synthetic peptides • KXXK motif

LDL, long established as the major plasma particle in the transport of lipids, is considered the chief causative agent in cardiovascular diseases. LDL particles have been the subject of extensive study (1–6) that focused on commonly recognized properties of apo B100 as a lipid vector. A few "out-of-the-box" studies in 1980s and early 1990s suggested that apo B100 is involved in signal transduction pathways (7, 8), including regulation of immune response (9, 10). At present, numerous studies support a role for LDL in signaling (11–15). The function of LDL as a transporter of viral materials, including nucleic acids, in the plasma was documented (16–23); however, an explanation for this function at the molecular level has yet to be provided.

Low density particles composed of lipid, apo B100, RNA, and core protein of hepatitis C virus (*hcv*), termed lipo-viro-particles, were reported in the plasmas of individuals infected with *hcv* (17, 19, 21). These particles continue to be studied as a source of persistent, chronic infection. In addition, several reports have suggested that the *hcv* and other *Flaviviridae* viruses may negotiate cell entry via the

LDL and VLDL DNA binding studies were conducted independently at Baylor College of Medicine under a Sponsored Research Agreement awarded to J. Guevara, Jr. by AraGene, Inc. at the AraGene, Inc. laboratory; at the Department of Integrative Biology and Pharmacology, UTHSC Houston under a research contract to D. Loose by Aragene, Inc.; and Biophysics Research Laboratory at UTB. Synthetic peptide studies were conducted at UTB. Studies at UTB were supported by grants F49620-99-1-0327 (AFOSR, PI: J. Guevara), and FA 9550-05-1-0472 (AFOSR, PI: A. Hanke), and SCORE pilot project 1SC2GM081218-01, 8SC2NS063952-02 (NIH, PI: N. Guevara). Its contents are solely the responsibility of the authors and do not necessarily represent the official views of the National Institutes of Health or other granting agencies.

Manuscript received 18 October 2009 and in revised form 16 February 2010.

Published, JLR Papers in Press, February 16, 2010
DOI 10.1194/jlr.M003277

Abbreviations: CBB, Coomassie brilliant blue; *dng*, Dengue virus; EMSA, electrophoretic mobility shift assay; GFP, green fluorescence protein; *hcv*, hepatitis C virus; HCMV, human cytomegalovirus; HSV, herpes simplex virus; *irf*, interferon regulatory factor; NLS, nuclear localization signal sequence; SUV, Small unilamellar vesicle; TA, Tris-acetate; UL122, herpesvirus 5 (HSV) immediate-early transcriptional regulator protein; *wnlv*, West Nile virus; *ylfv*, yellow fever virus.

[2] Present address of N. Prashad: Nanospectra, Inc., 8285 El Rio Street, Houston, TX 77025.
[3] Present address of B. Ermolinksy: Department of Biological Sciences, Center for Biomedical Studies, University of Texas Brownsville/Texas Southmost College, Brownsville, TX 78520.
[4] Present address of J. W. Gaubatz: Department of Medicine, Section of Atherosclerosis and Vascular Medicine, Baylor College of Medicine, One Baylor Plaza, Houston, TX 77030.
[5] Present address of D. Kang: Department of Neuroscience Research, Mayo Clinic, Jacksonville, FL 32224.
[6] Present address of A. E. Schwarzbach: Department of Biological Sciences, University of Texas Brownsville/Texas Southmost College, Brownsville, TX 78520.
[7] Present address of D. S. Loose: Department of Integrative Biology and Pharmacology, University of Texas Health Science Center Houston, Texas Medical Center, Houston, TX 77030.
[1] To whom correspondence should be addressed.
e-mail: natalia.guevara@utb.edu

LDL B/E receptor (24, 25). These observations suggest possible links between LDL and viruses. *Flaviviridae* are single-stranded RNA viruses with a genome that encodes three structural proteins (capsid/core C protein, precursor membrane protein, and an envelope E protein) and seven nonstructural proteins (NS1, NS2A, NS2B, NS3, NS4A, NS4B, and NS5) (26). The genome is encapsulated in a sphere that includes multiple copies of the capsid/core protein. It is therefore possible that an analog sequence of the B/E receptor ligand (27, 28) is present in the structural proteins of these viruses.

In previous reports, we showed that human LDL binds DNA and RNA in vitro (18, 20) and that highly purified LDL can be used to transport and deliver plasmid DNA to the cell nucleus. We surmised that the capacity of LDL and VLDL to bind nucleic acids is likely based on the presence of regions in the apo B100 molecule that display sequence similarities to known nucleic acid-binding domains (29). Based on the location of arginine and lysine clusters and other motifs, five potential DNA binding domains, 11 potential KH domains of the heterogeneous nuclear ribonucleoprotein K (30, 31), and numerous bipartite nuclear localization signal sequences (NLS) were identified in the apo B100 primary structure (18, 20). One candidate DNA-binding region is contained in the first 100 N-terminal residues of the apo B100. Several sequence motifs also present in the DNA-binding domains of interferon regulatory factors (29), the interferon regulatory factor (*irf*s), are located in this region.

In this report, we explore the hypothesis that apo B100 and apo E have structural and functional similarities to viral DNA-binding proteins. We focus on two candidate nucleic acid-binding regions: N-terminus of apo B100, residues ^{0014}Lys-Ala^{0096} (Region 1) and the section encompassing the known B/E-receptor ligand of apo B100, residues ^{3313}Asp-Thr^{3431} (Region 2) (32,33). Sequences of these regions are compared with viral nucleic acid-binding proteins, the capsid/core proteins. The apo B100 Region 2 sequence is compared with the NS3 proteins of the *Flaviviridae* viruses [Dengue (*dng*), West Nile (*wnlv*), yellow fever (*ylfv*), and hepatitis C] (34, 35) and to UL122 protein from human cytomegalovirus (HCMV) (36). In addition, we expand our comparison of Region 1 to human *irf* proteins. Primary structure similarities strongly support these two regions of the apo B100 molecule as nucleic acid-binding domains in apo B100. We also analyze similarities between the receptor ligand region of apo E (Leu^{151}-Arg^{278}) and *dng* capsid proteins and demonstrate DNA-binding capacity of purified apo E. Our hypothesis compels us to consider that LDL and LDL-related particles, intermediate and very low density particles, are involved in transporting nucleic acids, and this capacity is imparted by specific regions of the apo B100 as well as apo E.

Here we present additional evidence that LDL and VLDL have the capacity to bind DNA. Further, LDL can be used to transfect a variety of cell types in vitro and in vivo. Based on the results of experimental studies utilizing synthetic peptides from Regions 1 and 2 of apo B100, we conclude that this capacity is mediated by elements in the apo B100 primary structure similar to viral proteins.

METHODS

Chemicals

All chemicals were of highest quality available. Water of 18.2 MΩ·cm resistivity was used throughout these studies. Tap water was passed through a mixed-resin filter, distilled, and filtered using a Barnstead E-pure system. Molecular biology grade Agarose was purchased from Fisher Scientific, Inc. PBS was obtained from MediaTech, Inc., Herndon VA, or other chemical suppliers. Tris-acetate (TA) buffer, DNA sequence grade, was obtained from TECNOVA, Inc. Nucleic acid sample loading buffer was from Bio-Rad, Inc. BOBO1™-iodide (B-3582) and Cell Tracker™ CM-DiI (C-7001) fluorescence dyes, and Lipofectin™ were purchased from Invitrogen, Inc. Synthetic peptides, of 95% or greater purity by HPLC analysis, were purchased from GenScript, Corp.. Plasmid vectors, pCMV β-Gal, pEGFP-N1, and pEGFP-N2, were from ClonTech, Inc. Plasmids, phMGFP, pGL2-Control, pCMVTNT®, and restriction enzymes *Stu*I and *Hin*dIII were obtained from Promega, Inc. Cell culture media, DMEM, and HyQ-RPMI 1640 were obtained from MediaTech, Inc. and Thermo Fisher Scientific, Inc. Transfection Reagent 1, DOTAP: DOPE (1:1) was purchased from Avanti Polar Lipids, Inc. QIAamp DNA Mini kit was obtained from QIAGEN, Inc. PCR reagents were obtained from Roche Biochemicals, Inc. DNA Molecular Weight standards were purchased from Roche Applied Science, Inc.

Isolation of plasma lipoproteins

Human. Highly purified preparations of human plasma LDL were obtained from Invitrogen, Inc. and Athens Research and Technology, Athens, GA. LDL was also isolated from human plasma by sequential ultracentrifugation in NaBr solutions yielding the 1.019–1.05 g/ml density range of LDL fraction (6). Single donor plasma with sodium EDTA added at time of collection was obtained from Innovative Research. Typically, purified preparations of LDL were dialyzed in PBS containing 10 mM $MgCl_2$. LDL was than evaluated for purity using SDS-PAGE, and tested for DNA binding capacity using electrophoretic mobility shift assay (EMSA). Once DNA binding capacity of the LDL preparation was confirmed, it was frozen drop-wise in liquid nitrogen and stored in aliquots of about 200 μL in liquid nitrogen until needed. Highly purified, delipidated apo E was purchased from Athens Research and Technology, Inc.

Rats. Female Sprague-Dawley rats, 8–10 weeks old, were obtained from Harland Laboratories, Inc. Animals were housed in the National Institutes of Health-accredited facilities in the University of Texas Health Science Center and Baylor College of Medicine. All animals were treated in accordance with the Guide for the Care and Use of Laboratory Animals published by the U.S. National Institutes of Health (NIH publication no. 85-23, revised in 1996). All animal protocols were approved by the Animal Welfare Committees at the University of Texas Health Science and Baylor College of Medicine.

Rat plasma was used to purify LDL. To obtain blood, animals were first sedated using inhalation anesthetic metaphane. This was followed by an injection of a combination anesthetic containing ketamine (42.8 mg/ml), xylazine (8.6 mg/ml), and acepromazine (1.4 mg/ml) in PBS. Blood was then collected by heart puncture using a 5 ml syringe containing 50 μl of 100 mM EDTA. Approximately 4–5 ml of blood was collected per animal. Samples were pooled and centrifuged at 400 rpm for 20 min. LDL was isolated using equilibrium ultracentrifugation in preformed gradient of KBr. Collected plasma, 9–10 ml from six rats, was diluted to 12 ml with saline, then the density of the sample was adjusted to 1.21 g/ml with KBr. Plasma was transferred to centrifuge

tubes of SW 40 Ti swinging bucket rotor (Beckman), 4 ml per tube, overlaid with KBr solutions of the following densities: 1.063 g/ml (3.0 ml), 1.02 g/ml (3.0 ml), and 1.006 g/ml (2.5 ml). Samples were next centrifuged at 39,000 rpm for 60 h at 4°C. Seven fractions were collected from each tube, starting from the top of the centrifuge tube, and similar fractions from different centrifuge tubes were pooled then dialyzed against PBS. Protein concentration was routinely determined using modified Lowry method (18), and SDS-PAGE (2–12%) was performed. LDL fraction was identified by presence of apo B100 band.

EMSA

An aliquot of plasmid DNA digested using restriction enzymes was placed at the bottom of a microfuge tube; next, a buffer solution containing 25 mM TA, pH 7.6, and 10 mM $MgCl_2$ was added. An aliquot of purified lipoprotein (LDL, VLDL, apo E) or synthetic peptides was then added; the cocktail was stirred gently for less than 5 s and incubated for 30 min at 37°C. Sample loading buffer (Bio-Rad) was then added at a 1:5 (v/v) ratio to the polypeptide-DNA mix. Next, each sample was mixed and subjected to electrophoresis using 0.5–0.8% agarose gels in TA buffer at 100 V. Aliquots of nucleic acid, synthetic peptides, and lipoprotein were each analyzed in separate lanes as controls. DNA bands were visualized using ethidium bromide. Peptides and proteins in lipoprotein particles were visualized using Coomassie brilliant blue R-250 (CBB).

Cells

All cell types used in these studies were obtained from the American Type Culture Collection Organization. Cells were kept in liquid nitrogen until needed and then grown according to American Type Culture Collection protocols.

Several cell types, NIH/3T3 (mouse embryonic fibroblast cell line, CRL-1658™), CHO (chinese hamster ovary, CCL-61™), MCF7 (human breast adenocarcinoma cell line, HTB-22™), Hep G2 (human hepatocyte carcinoma cells, HB-8065™), and HeLa (human cervix epithelial adenocarcinoma cell line, CCL-2™), were used for LDL- and apo B100 synthetic peptide-mediated transfection. Cells were grown and maintained in media as follows: HeLa, Hep G2, MCF7, and NIH/3T3 cell types were in DMEM supplemented with 10% FBS, 100 units penicillin G-sodium, 100 units/ml streptomycin sulfate, and 250 ng/ml amphotericin B. CHO cells were in RPMI-1640 containing 10% FBS, L-glutamine, and 100 units penicillin G-sodium, 100 units/ml streptomycin sulfate, and 250 ng/ml amphotericin B. Cells were maintained at 37°C in an atmosphere of 5% CO_2 in a humidified incubator. Typically, cells were grown in culture plates (with or without glass cover slip in wells) to 60–70% confluence (20). Prior to transfection, the medium was removed, and cells were washed thrice with PBS. Cells were then incubated for a minimum of 2 h but not more than 4 h in FBS-free medium.

Dual label experiments were conducted using Hep G2 cells. The cells were grown overnight as described above on FBS-coated cover slips to enhance attachment. Cells were next washed with PBS and incubated in FBS-free medium for 4 h, then incubated for 3 h in 200 µl of transfection solution containing FBS-free DMEM, 10 mM $MgCl_2$, and preformed complexes of BOBO-1-labeled pCMV β-Gal plasmid DNA (3 µg), and either 15 µL of CM-DiI-labeled Lipofectin™ or 60 µg of CM-DiI-labeled LDL. The cell-coated cover slips were then removed, washed in PBS, and fixed in 4% paraformaldehyde for 10 min at 4°C. Each cover slip was then inverted over a well of a hanging drop slides containing PBS and viewed using an Olympus Model BH-2 fluorescent microscope.

Similar methods were used to study LDL-mediated transfection of CHO, NIH3T3, and HeLa cells using BOBO-1-labeled plasmid DNA. CHO and NIH3T3 cells were grown on cover slips and transfected using LDL complexed to BOBO-1-pEGFP-N1 DNA as described above, except LDL was not labeled. The cover slips were recovered at different periods and were inverted over on well slides containing PBS without paraformaldehyde treatment. Cell images were obtained using a LUMAM™ EPI-Fluorescent microscope. Similarly, HeLa cells were grown in Costar® multi-well, flat bottom polystyrene plates and transfected using solutions containing LDL complexed to BOBO-1-pCMVTNT DNA. Results of HeLa cell transfection were documented using a Zeiss Axiovert 25 microscope.

Nonlabeled LDL complexed to the nonlabeled pEGFP-N1 plasmid was used to transfect HeLa, MCF 7, CHO, and NIH/3T3 cell types as described above, and green fluorescence protein (GFP) expression was documented using a LUMAM™ fluorescence microscope with a GFP filter.

HeLa cells were used also to ascertain the transfection capacity of two sets of synthetic peptides. Cells were grown as routine, preconditioned in FBS-free DMEM for 4 h, washed thrice with PBS, and 400 µl PBS supplemented with 10 mM $MgCl_2$, containing either the synthetic peptides or peptide/DNA complexes was added. Cells were incubated at 37°C as described in Methods for 30 min, then washed, and Trypan Blue dye in PBS was added.

Noncovalent labeling of plasmid DNA with BOBO-1

Labeling of DNA with BOBO-1™-iodide was accomplished according to the methods described by the vendor (Molecular Probes dimeric cyanine nucleic acid stains) with minor modification. Briefly, 3 µl of 10 µM dye (1 mM stock solution diluted 1:100 with ethanol) was added to 10 µg of DNA at a concentration of 0.5 µg/µl in PBS, and the solution was incubated at ambient temperature for 1 h.

Labeling of Lipofectin™ and LDL with CM-DiI

Labeling of Lipofectin™ and LDL with Cell Tracker™ CM-DiI was performed according to the methods described by the vendor (Molecular Probes). Transfection agents were labeled by adding 1 µl of 20 µg CM-DiI/ml in ethanol (stock solution) to 100 µL of Lipofectin (undiluted reagent) or LDL (1.5 mg/ml by protein), and the mixture was incubated for 1 h at ambient temperature. Unreacted dye was removed using a Sephadex G-25 column.

Liposome preparation

Transfection Reagent 1 (10 mg, Avanti Polar Lipids, Inc.) was dissolved in 2 ml of a sterile buffer solution of 0.9% NaCl, 5.0% glucose, and 10% sucrose. The suspension was placed in a 37°C water bath for 10 min and vortexed to disperse the opaque lipid vesicles. Small unilamellar vesicles (SUV) were then formed by sonicating the mix for about 3 min. The transparent SUV mix was concentrated to approximately 11 mg/ml using an Amicon/Microcon filter concentrator with a YM-3 membrane (Sigma, Inc.). The solution was then sterilized through a 0.22 micron filter (Millipore, Inc.).

Transfection solutions

All LDL preparations used in this study were shown to bind DNA in EMSA prior to cell transfection experiments. Plasmids pCMV β-Gal, pEGFP-N1, pEGFP-N2, phMGFP, pGL2-Control, and pCMVTNT® bound LDL in a similar manner.

LDL. For cell transfection, purified LDL was added to the microfuge tube containing DNA and PBS with 10 mM $MgCl_2$. The mixtures were then incubated at 37°C for 30 min before use. Typically, 20–40 µg of LDL protein was complexed with 1.0 µg DNA.

Lipofectin™. Ten microliters of reagent in 100 µl culture medium was combined with 100 µl culture medium containing 10 µg DNA. The solution was then stirred gently and incubated for at least 30 min at room temperature.

Liposome. Transfection Reagent 1 was prepared as described above. The SUV preparation was combined with plasmid DNA (10:1) in TE buffer and incubated at ambient temperature for 5 min before use.

Synthetic peptides. Amino acid sequences of the peptides are listed in Table 1 (Region 1) and Table 3 (Region 2). Peptides were received in lyophilized form and 1 mg/ml solutions were prepared in PBS/10 mM $MgCl_2$ by vortexing. Solutions were frozen drop wise in liquid nitrogen and stored at −80°C until use. Aliquots were thawed and sterilized using a 0.2 micron filter immediately prior to use. In EMSA, plasmid DNA was mixed with 3, 6, and 12 µg of peptide individually or in a mixture representing a region of apo B100. Peptides were first mixed in equal amounts (v/v) and incubated at 37°C for 30 min. The peptide mix was then added to the DNA in a microtube after which PBS/$MgCl_2$ buffer was added and the cocktail was mixed by repeated drawing into the pipette tip.

Animal transfection experiments

Two separate animal studies were conducted. In one study at Baylor College of Medicine, 12 rats were used to determine GFP expression in different tissues after human LDL- and rat LDL-mediated transfection. Prior to transfection, both human LDL and rat LDL were shown to bind DNA in a similar manner using EMSA (data not shown). Animals were separated into three sets. Transfection cocktails were introduced via multiple ports, including those typically associated with viral infections such as HIV and HSV. Each animal was given an intravenous injection in the femoral vein and subcutaneously; also, inoculants were introduced into the peritoneal cavity, applied into the pharynx, nasal cavity, and rectum. Animals in Set 1 (control) were inoculated with linearized pEGFP-N1 plasmid DNA in which the HCMV I.E. promoter sequence was interrupted by digestion with *Hin*dIII, 5 µg of DNA in 100 µL of PBS/10 mM $MgCl_2$ per site. Set 2 animals were inoculated with a preformed complex of purified rat LDL and pEGFP-N1 plasmid, linearized using Stu I. Set 3 animals were inoculated using a cocktail mix containing human LDL and linearized pEGFP-N1 plasmid (100 µg of LDL protein and 5 µg of DNA in 100 µL of PBS/10 mM $MgCl_2$ per site). One animal from each set was euthanized as described above (Isolation of Plasma Lipoproteins section) on days 2, 5, and 7; tissues were excised and immobilized in O.C.T. compound and frozen using liquid nitrogen. The immobilized tissue samples were sectioned using a cryomicrotome. Sections (5–8 µm thick) were fixed for 30 min in 4% paraformaldehyde and analyzed for expression of GFP by fluorescent microscopy. Animals scheduled for day 9 study were spared, because GFP expression was not observed in tissues harvested on days 5 and 7.

In separate experiments performed at UTHSC, four animals were transfected with either pGL2-Control alone or pGL2-Control complexed to LDL, cationic liposome (Transfection Reagent 1), or to a mixture of LDL and liposome and distribution of the luciferase gene in rat tissues was determined by PCR.

Rats were anesthetized with ketamine/xylazine (200 mg/10 mg per 1 kg animal weight injected intraperitoneally) and a small incision was made through the skin of the inner thigh to expose the femoral vein. Injection of plasmid DNA was made with a 30 gauge needle directly into the femoral vein. After the injection, pressure was applied to the puncture to avoid leakage and was continued until coagulation occurred. The skin incision was closed with a wound clip. All animals were injected with mixtures containing 200 µg of pGL2-Control plasmid DNA (Promega, Inc.). The control animal, rat1, was injected DNA in Tris-EDTA buffer. Test rat2 was injected with pGL2-Control complexed with LDL (1:5) in 10 mM Tris (pH 7.5), 40 mM NaCl, 1 mM EDTA, 1 mM DTT, and 4% glycerol. Rat3 was injected with pGL2-Control complexed with the liposome (1:10, as described above) and rat4 was with cocktail composed of pGL2-Control: LDL: liposome (1:1:7). Animals were anesthetized with ketamine/xylazine and decapitated 24 h after the transfection injections were administered. Tissue samples were collected from heart, lung, liver, brain, kidney, and spleen, weighed, and immediately frozen in liquid nitrogen. Liquid N_2 was added to the sample (25 mg of each tissue, except 10 mg of spleen was used) in a cold mortar and ground to a fine powder using a chilled pestle. Tissues were digested with Proteinase K for 24 h at 56°C; DNA was then extracted from each tissue using the QIAamp DNA Mini kit (QIAGEN, Inc.) as described in the QIAGEN Handbook of Protocols. Presence of the luciferase gene was confirmed via PCR using reagents from Roche Biochemicals, Inc., and a primer set, 5′agcaactgcataaggctatg and 3′gttggtactagcaacgcact obtained from Genosys Biotechnologies, Inc. Reactions were performed in a Perkin Elmer DNA Thermal Cycler Model 480.

Fluorescent microscopy

Microscopy of Hep G2 cells and animal frozen tissue sections was performed using an Olympus model BH-2 fluorescence microscope equipped with a Hamamatsu 3 CCD model C5810 camera. The LUMAM™ EPI-Fluorescence microscope (LOMO America, Inc.) equipped with an Optronics MacroFire® 2.0 CCD camera and the Zeiss Axiovert 25 microscope with the Optronics MicroFire CCD camera were used to obtain all other cell images. The following filter sets were used: a fluorescein (FITC/TRITC) no. 51004V2 cube, a Chroma HQ-GFP NB 710 cube no. 41020 (Chroma Technology, Brattleboro, VT), and an Olympus dichroic DM500 (BP490) filter.

Image processing

Adobe Photoshop CS version 8 software and full-frame images of the same field of view of equal size and dimensions were used to create merged overlay images. Images obtained at emission spectrum of 505–515 nm were used as background, and bright light images or red region images were overlaid at 50% transparency.

Sequence alignment

Selection of protein sequences was based on the association of LDL/VLDL and *Flaviviridae* viruses (24, 25) in human plasma, observations regarding colocation of apo B100 and HCMV DNA in arterial wall (37, 38), our previous reports on the similarity of apo B100 to *irf* proteins, and on preferential binding of LDL to CMV promoter-containing plasmids (20). The apo E LDL receptor ligand sequence spanning residues Leu^{151} to Arg^{278} was also included. All protein sequences were obtained from the National Institutes of Health protein database and saved as simple text documents. The capsid protein sequences for *dng* versions 1–4, *hcv*, *wnlv*, *ylfv* virus, bovine viral diarrhea virus, and NS3 helicase sequences were obtained from their respective polyprotein files in the same database. Rather than identifying all clusters of group-related amino acids, we first focused our efforts on two types of clusters. The letter symbols for amino acids arginine (R), lysine (K), histidine (H), proline (P), cysteine (C), and glycine (G) were highlighted in each protein sequence file to locate basic amino acid clusters such as the apo E LDL receptor ligand "RKXRKR", and motifs common to nucleic acid binding domains as well as structurally important motifs such as "PG" and "GXXG". Se-

JOURNAL OF LIPID RESEARCH ASBMB

quences containing these features were then aligned and group-related amino acids in multiple sequences were highlighted to further assess similarity. Two regions in the apo B100 sequence were selected for these analyses: Region 1 spans the N-terminus from Glu^{0013} to Pro^{0140} and Region 2 includes residues Asp^{3313} to Arg^{3500}. Each of these apo B100 regions contains at least one basic amino acid cluster. Different options for multiple sequence alignment were also evaluated using T-COFFEE (http://www.bioinformatics.nl/tools/t_coffee.html).

Sequence comparison was also performed using two recognized algorithms for sequence similarity searches, SSEARCH and PSI-BLAST. The entire sequences of Regions 1 and 2 of apo B100, as well as their fragments and expanded versions, were used as query sequences. SSEARCH of UniProtein Knowledgebase, and UniProtKB/SwissProt databases was performed at the EBI site (http://www.edi.ac.uk/Tools/fasta33/index.html) using all available BLOSUM matrices (BLOSUM 50, 62, and 80) and default or weaker gap penalties (e.g., BLOSUM 62 has -11/-1 for gap opening/gap extension as default setting). PSI-BLAST searches were conducted at the NCBI website (http://blast.nchi.nlm.nih.gov/Blast.cgi). Databases of various sizes were searched, each with various search settings such as scoring matrices (BLOSUM 45, 62, and 80) and PSI-BLAST thresholds. Several iteration steps (3–5 times) were performed until the search did not result in any new additional finds.

RESULTS

DNA-binding

Present studies expand data on the capacity of LDL to bind HCMV promoter-containing plasmids and to transfect cells in vitro (18, 20); also, the latter property is newly demonstrated in vivo. In **Fig. 1** (upper panel), DNA-binding capacity of human lipoproteins, VLDL, LDL, and HDL, is illustrated. LDL samples from two donors are shown (donor A, lanes 1–5, and B, lanes 6–10); both samples had similar mobility in CBB-stained gel (middle panel) and bound the pCMV β-Gal plasmid in almost identical fashion (upper panel). VLDL, although a larger apo B100-containing particle, displays higher electrophoretic mobility compared with LDL due to differences in both lipid and protein contents (6, 39). Results shown in Fig. 1 (lanes 14-15, donor B only) indicate that VLDL binds to plasmid DNA in a concentration-dependent manner. Further, the mobility pattern for VLDL in the EMSA differs from the pattern seen for LDL. At lower VLDL concentrations, bound DNA is seen in a band of higher electrophoretic mobility (lanes 12–13); the shift toward lower mobility region is observed at increased VLDL protein/DNA ratio (lanes 14–15) in the upper panel. In separate experiments, high purity, delipidated apo E was used to determine whether it contributes to the VLDL/DNA binding. Apo E binding to plasmid DNA (Fig. 1, lower panel) suggests that both apo B100 and apo E may determine the observed EMSA pattern for these particles.

Only apo B100-containing lipoproteins bound DNA in our studies. HDL, which lacks apo B100, did not influence plasmid mobility, lanes 16–18. Protease-treated LDL lost its capacity to bind DNA in EMSA (not shown). Hence, apo B100 is essential for DNA binding to lipoproteins.

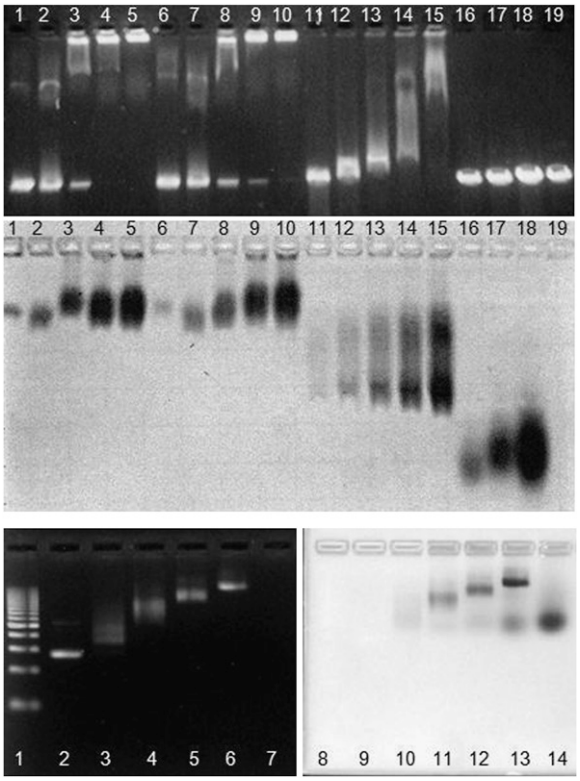

Fig. 1. EMSA of human lipoproteins binding to linearized pCMV β-Gal. Upper panel: Ethidium bromide-stained gel, 0.75% agarose in TA buffer, pH 7.6. Lanes 1–10: LDL binding to 1.0 μg of pCMV β-Gal linearized using *Hin*dIII. Lanes 1–5, LDL from donor A, 2.5, 5, 10, 20, and 30 μg by protein, respectively; lanes 6–10, LDL from donor B, same protein amount as in lanes 1–5. Lanes 11–15: VLDL (from donor B) binding to same plasmid DNA; 5, 10, 20, 30, and 60 μg of VLDL protein, respectively. Binding of LDL and VLDL to DNA is evident by formation of lower-mobility band and decrease in the amount of free plasmid as the concentration of lipoproteins increases. HDL from donor B did not bind to the plasmid at amounts of 10, 20, and 40 μg of HDL protein (lanes 16–18). Plasmid DNA alone is shown in lane 19. Middle panel: The same gel stained with CBB dye. Bottom panel: Ethidium bromide-stained 0.8% agarose gel is shown in the left image. Lane 1: DNA ladder; lane 2: 0.8 μg phMGFP plasmid; lanes 3–6: binding to the same amount of plasmid by 1.8, 3.6, 5.4, and 7.6 μg, respectively, of >95% pure, delipidated apo E; lane 7: 7.6 μg apo E alone. Image on right is the same gel stained with CBB.

Sequence comparison analysis

Highlighting group-related amino acids in sequence files discussed in Methods revealed the location of clusters and motifs that were then used to align multiple sequences.

Region 1, the N-terminal sequence of apo B100

Capsid proteins of the flaviviruses and DNA binding domains of *irf* proteins are rich in arginine and lysine amino acids. Arg/Lys-rich clusters are located near the N-termini of apo B100, *hcv*, *ylfv*, *dng 1–4*, and *irf* proteins 1, 2, 5, 6, 8, and 9. In the sequences of *irf* proteins 3, 4, and 7 and *wnlv* and *bvdv*, Arg/Lys clusters are located distal to the first 20 N-terminal residues.

Flaviviruses are thought to gain cell entry via the LDL B/E receptor (24, 25). The well-established B/E receptor ligand region in apo E is an Arg/Lys-rich cluster, ^{0141}LRKLRK^{0146}

(27). The critical residues in binding/docking to the receptor are lysine residues 0143 and 0146, which are located on the hydrophilic side of an amphipathic helix (27). Replacing either lysine with arginine (as RXXK or KXXR) does not affect binding affinity; however, arginine substitution of both sites (RXXR) reduces binding by almost 70% (27).

The R/K-X-X-R/K is a multi-functional motif (including RXXR) essential in both protein-protein interactions, including nuclear entry (NLS sequences) and protein-nucleic acid interactions (40–43). A comparison of the R/K clusters in Region 1 of apo B100, flaviviral capsid proteins, and *irf* DNA binding domains is shown in **Table 1**. The N-terminal cluster of apo B100 contains three renditions of the R/K-XX-R/K motif as RXXH, KXXR, and HXXK (see column 1); apo E N-terminus has HXXK, two RXXR, and one KXXK; there are three copies in *hcv* (KPQR, RKTK, KTKR); one as RXXR in *ylfv*; and all versions of Dengue capsid proteins are replete with this motif, bipartite NLS sequences, and the R/K-X-R/K-X-R/K motif.

Arginine, in RXRXR and RXXR motifs, is the predominant basic amino acid in the N-terminal clusters of the *irf* proteins. Only the RXXR low affinity B/E receptor ligand motif is present in the N-termini of DNA binding domains of *irfs 5*, *6*, *8*, and *9*. The high-affinity B/E receptor ligand motifs (27) KXXK, KXXR, and RXXK, absent in the N-terminal R/K clusters of *irf* proteins, are present in their DNA binding and NLS motifs located in the C-terminal region of these domains (44).

The motif K/R-XXX-K/R shown in column 3 and present in the sequences of apo B100 Region 1, *bvdv*, *hcv*, and *irf*s is repeated several fold in the *irf* proteins. Another motif that appears in most of these proteins is the Φ Φ Φ-K/R motif (Φ, hydrophobic residue); it is also highlighted in column 3. In *irf*s, these motifs have been shown to interact with the backbone phosphate moieties of the nucleic acid (45).

Analogs of the K/R-XXX-K/R motif, shown in column 4, are part of the NLS sequence located before the metal-binding sequence of the *irf* proteins (45). The apo B100 sequence, NPEGKALLK is very similar to the sequence QPEGRAWAQ in *hcv* capsid protein. In *irf*s, the NPEG appears as EPDP and is separated from the K/R-XXX-K/R motif by a tripeptide sequence, KTW, missing in apo B100, and two viral capsid proteins, *bvdv* and *hcv*. An analog of the apo B100 sequence, KKTKNSEEF, is contained in the *bvdv* as TKSKNTQDG and as "NKSSEF" in *irf* 9.

A PG motif is also located near the N termini of apo B100, *hcv*, and *irf* proteins 1, 2, 4, 5, 6, 8, and 9 but not 3 and 7 (column 2, Fig. 1). The PG motif was used as a reference point for alignment and served in locating clusters of polar amino acids, also highlighted in column 2.

In *hcv*, the capsid/core protein is cleaved within a short stretch of hydrophobic amino acids, ^{0175}SIFLLALLS^{0183} (26). Analog sequences are also present in other flaviviruses. Three motifs contained in this region of the *hcv* capsid protein, shown in column 5, are also apparent in apo B100, ^{0132}GIISALLVP^{0140} (with 2 potential cleavage sites), ^{0148}QVLFL^{0152}, and ^{0158}NCS^{0160} (a potential N-glycosylation site).

Apo E similarity to Flaviviridae capsid proteins

A sequence alignment comparison of the apo E sequence containing the B/E receptor ligand, residues Leu^{151} to Arg^{278}, and the sequences of the four versions of *dng* was performed to identify analog elements. Results are presented in **Table 2**. The *dng1* and *dng3* proteins have three discrete Arg/Lys-rich cluster in their N termini, each containing a copy of the K/R-XX-K/R motif (underlined in columns 1 and 2). Additional analog sequences are highlighted in bold in column 2. A potential bipartite NLS sequence was identified in the carboxy-terminal region of the apo E molecule (column 3, Table 2).

In summary, the N-terminal region of apo B100, the LDL B/E receptor ligand region of apo E, capsid proteins of the several flaviviruses, and the DNA binding domain regions of the *irf* proteins appear to be analogs of each other, which suggests similar functions. For apolipoproteins, these similarities mean potential DNA-binding and nuclear translocation capacities. In turn, similarity of Flaviviridae capsid proteins to apolipoproteins may greatly facilitate ability of these viruses to penetrate cells.

Region 2, the putative helicase domain of apo B100

The apo B100 sequence extending from Asp^{3313} to Ser^{3458} was predicted to bind DNA and mediate cell entry due to the presence of both Arg/Lys-rich clusters and the accepted B/E receptor ligand sequence, ^{3353}KLEGTTRLTRKRGLKLA^{3369}. Based on the apparent preferential binding of LDL to plasmids containing the HCMV IE2 promoter (20), this region of the apo B100 sequence was compared with the sequence of the HSV5 UL122 protein, which binds to the CMV promoter (36). The apo B100 Region 2 sequence was also compared with the NS3 helicase of the *Flaviviridae* viruses, *dng1*, *wnlv*, and *ylfv*, because an Arg/Lys-rich cluster was located within the NS3 sequence by highlighting of the arginine and lysine residues in their precursor polyprotein sequences. The sequence alignment comparison of the NS3 helicase domains of the HSV5 UL122 and *Flaviviridae* NS3 to the proposed analog sequence in apo B100 is presented in **Table 3**. Apo B100 (residues 3316–3458) and UL122 (residues 276–420) share motifs KSS, LLSSSSSV, and GTTR. In column 3, a comparison of arginine/lysine-rich clusters of the NS3 helicases, e.g., ^{1685}REAIKRKLRT in *dng1*, and the analog sequence in apo B100 LDL B/E receptor ligand, ^{3359}RLTRKRGLK, is shown. In the NS3 helicases of *dng*, *wnlv*, and *ylfv*, the KXXR motif is part of the Walker A motif (34, 46), GXGKTRR. Analog sequences occur as GTTRLTR in apo B100 and as ASTGPRKKK in UL122 (Walker motifs are associated with nucleotide binding in kinases and helicases) (47). Flanking the Walker A motifs in the viral helicases are sequences of two β-sheet structures, e.g., QITVLDL and LRTAVLAP in *wnlv*. These are conserved in analog sequences SSSVIDA and LKLATALS in apo B100. The hydrophobic stretch, ^{3367}KLATALSLSNKFV, which follows the receptor ligand in apo B100, may be a legitimate analog to the sequence ^{1691}KLRTLILAPTRVV in *dng1* and other *Flaviviridae* helicases (35). The sequence alignments in columns 4 and 5

Table 1. Comparison of Amino Acid Clusters and Motifs of apo E, Apo B100 N-Terminus (Region 1), DNA-binding Domains of Interferon Regulator Factors and the capsid/core proteins of *Flaviviridae* viruses.

Protein	Arginine/Lysine Clusters (B/E receptor ligand)	Proline-Glycine Motifs and –OH and –NH2 Clusters	DNA-Phosphate Interacting Segment
apo E	RLASHLRKLRK	*RLLRDADDLQ	AVYQAGAREGAERGLSAIRER
apo B	CPKDATRFKHLRK	YTYNYEAESSSGVPG	DSRSATRINCKV******ELEVPQLCSFILKTS
bvdv			*IKSATRSYQRVFRWVHNRLD**********
hcv	MSTNGKPQRKTKR	NTNRRPQDVKFPG	GPRLGVRATRKT****WERSQPRGRRQPIPKAR
irf1	MPITRMRMR	PWLEMQINSNQIPG	NKEEMIFQIPWKHAAKHGWDINKD*AC**LFRSW
irf2	MPVERMRMR	PWLEEQINSNTIPG	NKEKKIFQIPWMHAARHGWDVEKD***APLFRNW
irf6	MALHPRRVRLK	PWLVAQVDSGLYPG	RDSKR*FQIPWKHATRHSPQQEEE**NT*IFKAW
irf8	MCDRNGGRRLR	QWLIEQIDSSMYPG	NEEKSMFRIPWKHAGKQDYNQEVD*AS**IFKAW
irf9	MASGRARCTRKLR	NWVVEQVESGQFPG	DTAKTMFRIPWKHAGKQDFREDQD***AAFFKAW
dng1	QRKKTGRPSFN*MLKRAR	VSTVSQLA	RFSKGLLSGQGPMKLVMAFIAFLR-**GILARWG
ylfv	GKTLGVNMVRRGVRSLS	NKIKQKTKQIGNRPG	LTGK***KITAHLKRLWKM*LDPRQG*LAVLRKV

Protein	NLS Sequence and Metal Binding Segment	Endopeptidase Cleavage Site
apo E		
apo B	KEVYGF*NPEG***KALLK**KTKNSEEFAAAM	PTYILNI*KRGIISALLVPPETEEAKQVLFLDTVYGNCS
bvdv	KDSKTKP*PDA///RKKGKT*KSKNTQDGLYHN	NKPQESRKKLEKALLAWAIIA****IVLFQVTMGENIT
hcv	*******QPEG***RAWAQPGYPWPLYGNEGLG	VNYATGNLPGCSFSIFLLALLSC*LTVPA*SAYEVRNVS
irf1	KAGE**KEPDPKTWKANFRCAMN*SLPDIEEVK	
irf2	KHQPGVDKPDPKTWKANFRCAMN*SLPDIEEVK	
irf6	KYQEGVDDPDPAKWKAQLRCALNKSR*EFNLMY	
irf8	KEGDKA***EPATWKTRLRCALNKS*PDFEEVT	
irf9	KEGD***TGGPAVWKTRLRCALNKSS*EFKEVP	
dng1	REISNMLNIMN***RRKRSVTMLLMLLPTALAF	**MLNIMNRRKRSVTMLLMLLP******TALAF*HLTTR
ylfv	RQGLAVLRKVKRVVASLMRGLSSRKRRSHDVLT	RSHDVLTVQFLILGMLLMT****GGVTLVR

Synthetic Peptides	B1-1.	^{14}KDATRFKHLRKYTYNYEAESSSGVPGTADSRSATRINCKVE^{54}
	B1-2.	^{55}LEVPQLCSFILKTSQCTLKEVYGFNPEGKALLKKTKNSEEFA^{96}

Apo E (153-174), human NP_000032; Apo B (0012-0160), human NP_000375; *bvdv* (141-160; 201-210; 222-239), bovine viral diarrhea virus 1, NP_040937; *hcv* (001-198), hcv, P29846; *irf*1 (001-0095), P10914; *irf*2 (001-095), P14316; *irf*6 (001-097), NP_006138; *irf*8 (001-096), NP_002154; *irf*9 (001-098), Q00978. Similarities are in bold and underlined. KXXK motifs in the amino termini of apo B100, *hcv* and *dng1*, and within the first 100 residues of *ylfv* are compared to the B/E receptor ligand, LRKLRK, in column 1. The motif appears as RXRXR and RXXR in *irf* proteins. In column 2, a stretch, rich in non-charged, polar amino acids, with a PG motif at the carboxyl end, is shown. The *irf* protein sequences in column 3 are highly homologous and two motifs, DVE and IFK, are conserved in *irf* proteins and as an analogue sequence, ELE, in apo B100. The sequence RSATR of apo B100 is conserved in *bvdv* as KSATR (column 3). Common motifs shown in column 4 include KE, PEG, KAxLK/R, NKNS, and EF. NLS motifs are in apo B100 as KKTK and in the viral proteins as Arginine/Lysine clusters. In column 5, a cluster of hydrophobic amino acids that include the LL motif, the endopeptidase ligand/substrate in the *hcv* core protein, is conserved in apo B100 and viral proteins but absent in *irf* proteins. Synthetic peptides of this region of apo B100 were shown to have the similar properties as those reported for the *hcv* and *wnlv* capsid/core proteins (38-42).

weakly suggest similarities between these proteins. Notably, the DEAD motif typical of helicases is not conserved in apo B100 but may be represented as DFNS.

Our method for sequence comparison analysis identifies weakly similar sequences that may be analogs of known proteins and therefore may perform similar functions. This algorithm reveals that apo B100 Region 1 sequence shares about 46% similarity and 22% identity with the DNA binding domains of the *irf* proteins and about 25% similarity and <10% identity with the viral capsid proteins. Sequence similarities between apo E and the *irf* proteins were <25%. The apo E sequence spanning ^{0155}Leu and ^{0248}Asp is 55% similar to the first 100 N-terminal residues of *dng1*.

Similarity searches using SSEARCH and PSI-BLAST algorithms were performed to probe the protein sequence databases for potential homologies and to further substantiate our observations. Although these algorithms find several matches to RNA- and DNA-binding proteins in the SwissProtein database, the E-value range for these matches is $1 < E < 10$ and is therefore not considered highly significant. All statistically significant homologs belong to several families of lipoprotein transport proteins of animals, and no significant viral homologs were revealed. Similar searches were performed with input sequences of the viral proteins included in Tables 1 and 3, and these resulted in the detection of viral sequences only.

LDL-mediated transfection of cells in culture

Different cell types, including HeLa, Hep G2, CHO, and NIH3T3, were transfected using LDL mixed with BOBO-1-labeled plasmid DNA containing the HCMV promoter as described in Methods. Typically, LDL-mediated transfection of HeLa, Hep G2, and NIH3T3 cells occurred rapidly after upregulation of the B/E-receptor via incubation of cells in FBS-free medium for 2–4 h; fluorescence was observed within minutes after LDL/BOBO-1-DNA mix is added to the medium. Almost 100% of HeLa cells shown in **Fig. 2A** were transfected within 30–45 min, and BOBO-1 fluorescence is seen predominantly in cell nuclei. In CHO cells, transfection occurred over an extended period for hours, not minutes (Fig. 2B). Also, fluorescence appeared to remain in the cytoplasm with little to none in nuclei. Few to no cells were transfected in all cell types by naked DNA (Fig. 2C).

In Hep G2 cells, two fluorescence dyes (CM-DiI for transfection agents, BOBO-1 for pCMV β-Gal DNA) were used to compare Lipofectin- and LDL-mediated transfection (Fig. 2D–K). All images were taken at 3 h after transfection. This time point was chosen for optimal transfection results using Lipofectin, which was delayed compared with

Table 2. Comparison of Amino Acid Clusters and Motifs of Apo E and the capsid/core proteins of *Flaviviridae* viruses.

Protein	B/E Receptor Ligand	Hydrophobic Region of Dengue	NLS Sequence Motif
	** *** *		* * * * *
apoE	LASHLRKLRKRLLRDADDLQKRLAVYQAGAREGAE	RGLSAIRE**RLGPLVEQGRVRAATVGSLAGQPL	RARMEEMGSRTRDRLD
	* * * * *	*	** ****
*dng*1	MINQRKKTGRPSFNMLKRARNRVSTVSQLAKRFS-	KGLLSGQGPMKLVMAFI*AFLRFLAIPPTAGILA	KREISNMLNIMNRRKR
*dng*3	MNNQRKKTGKPSINMLKRVRNRVSTGSQLAKRFS-	RGLLNGQGPMKLVMAFI*AFLRFLAIPPTAGILA	KKEISNMLSIINRRKK

Similar and analogue sequences in the apo E LDL receptor ligand region and dengue capsid proteins are indicated in bold and underlined. The K/R-XX-K/R motifs are identified by the asterisks above the letter symbols.

LDL-mediated DNA delivery. Uptake of label was not seen in cells given DNA only (not shown). Extracellular location of fluorescence can be seen in cells treated with labeled Lipofectin alone (Fig. 2D). These extracellular aggregates may result from Lipofectin interaction with cell debris or may form before its cell entry. In contrast, signal from labeled LDL is typically seen associated with cells (Fig. 2H). Micrographs E–G and I–K illustrate cellular uptake of dual labeled Lipofectin/DNA and LDL/DNA complexes, respectively. Red fluorescence of labeled Lipofectin (Fig. 2E) in the cytoplasm is more intense and not in discrete loci as seen for labeled LDL (Fig. 2I). Little or no red fluorescence is present in the nuclear spaces. BOBO-1 green fluorescence is seen in nuclei and cytoplasm of cells transfected with Lipofectin/DNA (Fig. 2F) and LDL/DNA (Fig. 2J). Dual color images (Fig. 2G, K) further emphasize colocation and separation of dyes suggested by the monochrome images.

LDL-mediated delivery of pEGFP-N1 DNA to cells was tested further by monitoring GFP expression in different cell types (Fig. 2, right panel, L–P). No dyes were used in these experiments. Fluorescence was not seen in controls where naked DNA was used (not included). Merged overlays of brightlight and fluorescence images in Fig. 2L show GFP expression in MCF7 cells at 2 h after transfection. Loci of apparent GFP synthesis are visible on the periphery of nuclei. GFP expression was seen in <10% CHO cells examined (Fig. 2M). Intense and uniform distribution of GFP expression was seen in NIH/3T3 cells at 18 h (Fig. 2N) and in HeLa cells at 1 h (Fig. 2O) and 18 h (Fig. 2P) post transfection. Nuclei devoid of GFP are clearly visible (Fig. 2P). In summary, images in Fig. 2 unambiguously demonstrate successful LDL-mediated intracellular delivery and nuclear translocation of dye-labeled DNA as well as GFP expression in transfected cells in vitro.

Animal studies

Rats inoculated with rat or human LDL/pEGFP-N1 mixtures via multiple ports were euthanized on days 2, 5, and 7 (Methods). However, GFP expression was not observed in tissues harvested on days 5 and 7. Photographs taken

Table 3. Common Amino Acid Clusters and Motifs in the Known B/E Receptor Ligand Region of apo B100, HSV 5 UL122 protein, and the NS3 Helicase Proteins of Dengue type 1, West Nile Virus, and Yellow Fever Virus.

Helicase Regions	-OH and –NH2 Rich	Leu/Ser Cluster	Arg/Lys Cluster (putative B/E receptor ligand region)
B100 3313	DFSFKSSVITLNTNAELFNQ	SDIVAHLLSSSSSVIDALQYKLE	GTTRLTRKRGL********KLATALSLSNKFV
UL122 276	SEEMKCSSGGGASVTSSSHH	GRGGFGGAASSSLLSCGHQSSGG	ASTGPRKKK*********SKRIS**ELDNEKVR
*dng*1 1629	VVTTSGTYVSAIAQAKASQE	EGPLPEIEDEVFRKRNLTIMDLH	PGSGKTRRYLPAIVREAIKRKLRTLILAPTRVV
wnlv 1659	VIMPNGSYISAIVQGERMDE	PIPAG*FEPEMLRKKQITVLDLH	PGAGKTRRILPQIIKEAINRRLRTAVLAPTRVV
ylfv 1641	ILVGDNSFVSAISQTEVKEE	GKEELQEISTMLKKGMTTILDFH	PGAGKTRRFLPQILAECARRRLRTLVLAPTRVV

Helicase Regions	Low Similarity Segment	DEXH-Like Motif
B100 3389	LTTKNMEVSVAKTT***KAEIPILRMNFKQELNGNTKSKP*TV****	*SSSMEFKYDFNS****SMLYSTAKGAVDHKL*SLES
UL122 349	FCTPNVQTRRGRV****KIDEVS*RM*FRN****TNRSLEYKNLPFT	*IPSMHQVLDEAIKACKTMQVNN*KGIQIIYTRNHEV
*dng*1 1714	VPIRYQT*TAVKSEHTGK*EIVDL*MCHAT*FTM****RLLSPVRV*	PNYNMII*MDEAHFTDP*ASIA*ARGYISTRVGMGEA
wnlv 1744	LPIRYQTSAVPR*EHNGN*EIVDV*MCHAT*LT****HRLMSPHRV*	PNYNLFV*MDEAHFTDP*ASIA*ARGYISTKVELGEA
ylfv 1727	LDVKFHT*QAF*SAHGSGREVIDA*MCHAT*LT****YRMLEPTRV*	VNWEVII*MDEAHFLDP*ASIA*ARGWAAHRARANES

Synthetic Peptides

B2-1. ^{3313}DFSFKSSVITLNTNAELFNQSDIVAHLLSSSSSVIDALQYKLE^{3355}

B2-2. ^{3356}GTTRLTRKRGLKLATALSLSNKFVEGSHNSTVSLTTKNMEVSVAKT^{3401}

B2-3. ^{3358}TRLTRKRGLKLATAL^{3373}

Apo B100 (3313-3458); UL122 (276-420), HCMV IE2 Human Herpesvirus 5, AAR31505; *dng*1 (1629-1785), Dengue virus type 1 helicase NS3 (1665-1794), AAQ19667;*wnlv* (1659-1815), West Nile virus helicase NS3 (1693-1824), NP_041724; *ylfv* (1641-1798), Yellow Fever virus NS3 (1678-1807), NP_041726. In columns 1 and 2, two analogue motifs are evident in the apo B100 and UL122 sequences, FKSS/MKCS, and LLSSSSSVI/AASSSLL. In column 3, a stretch rich in Arginine and Lysine residues is preceded by a short motif of Glycine and Serine/Threonine amino acids is in bold and underlined. At the carboxyl end of this cluster is a region of small hydrophobic and non-charged, polar residues with the RVV or a similar motif. In column 4, apo B100 motif SVAKT is analogous to TAVKS in *dng1* and SAVPR in *wnlv*. The TTKAEIP motif of apo B100 is conserved as TGKEIV in *dng1* and SGREVI in *ylfv*. Three apo B100 motifs, KAEIP, RMNFKQ, and NTKS, are similar to KIDEV, RMFRN, and TNRS in UL122. In column 5, the "DEXH-box", the signature motif of the *Flaviviridae* nucleic acid-unwinding helicases, is present as "DFNS" in the apo B100 sequence. Region 2 synthetic peptides of apo B100 bind to DNA, as demonstrated in EMSA (Fig. 4). However, helicase activity has not been verified for this region of apo B100. In addition, Region 2 synthetic peptides did not display transfection capacity in HeLa cells.

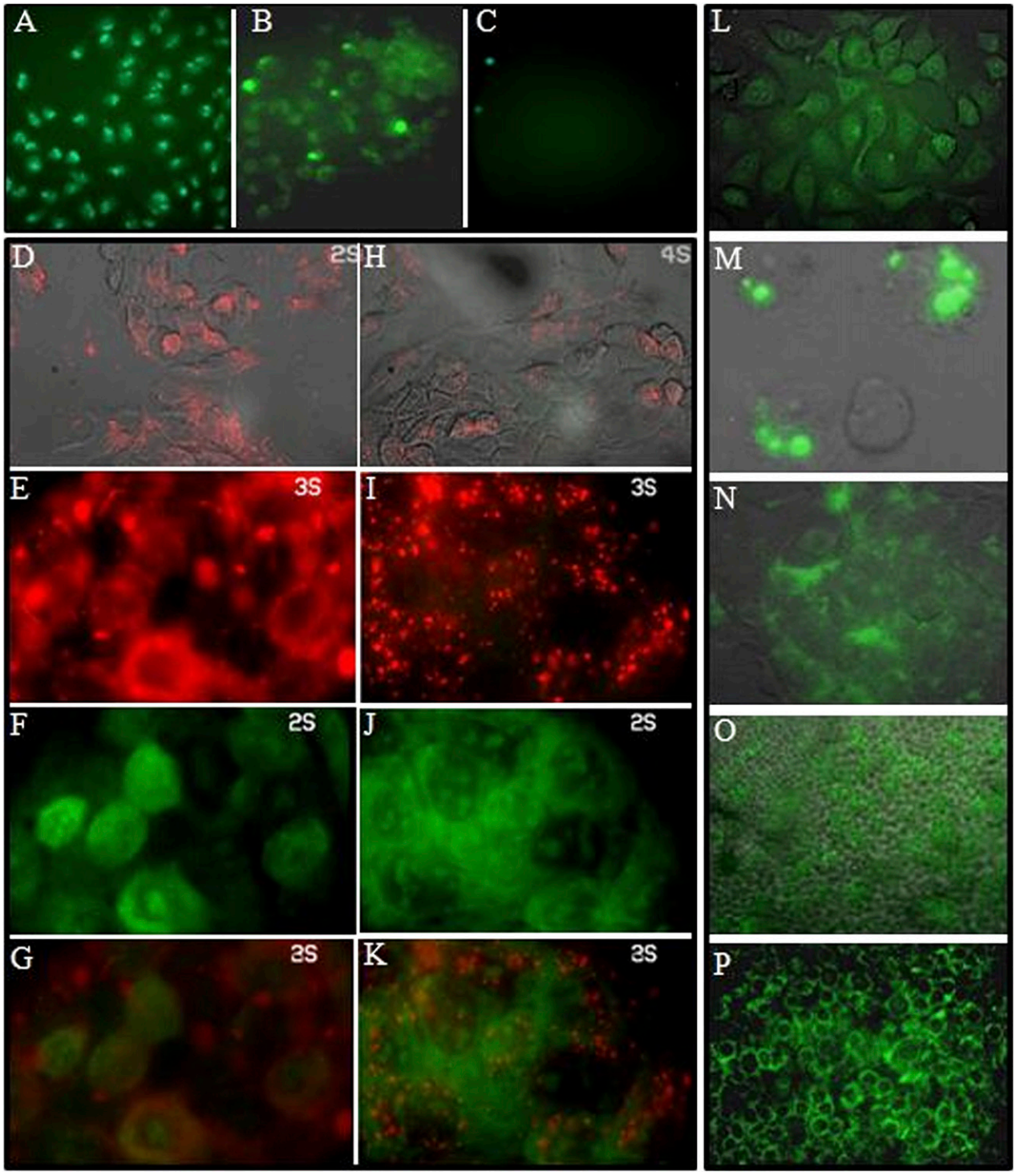

Fig. 2. LDL-mediated transfection of mammalian cell types with plasmid DNA containing HCMV promoter. Upper-left panel: Images A–C: LDL-mediated transfection of HeLa (A) and CHO cells (B) with BOBO-1-labeled pCMVTNT. HeLa cells given labeled plasmid alone are in C. Lower-left panel: Images D–K: HepG2 cells transfected using Lipofectin (D–G) and LDL (H–K) in dual label experiment. BOBO-1-labeled, linearized pCMV β-Gal combined with CM-DiI-labeled transfection agent was given toHepG2 cells (Methods). Images D (Lipofectin) and H (LDL) are brightlight and FITC filter overlay (merged) images of HepG2 cells treated with CM-DiI-labeled transfection agent alone. Images E–G show cells incubated with CM-DiI-Lipofectin/BOBO-1-pCMVβ-Gal, and images I–K show cells treated with CM-DiI-LDL/BOBO-1-pCMV β-Gal. Images E (Lipofectin) and I (LDL) obtained with the FITC filter show location of labeled transfection agents only. Images F (Lipofectin) and J (LDL) obtained using the GFP filter cube show labeled-DNA loci. Images G and K are merged images (D/E, Lipofectin) and (I/J, LDL) that show coloci and separate loci of labeled transfection agents and DNA. Right panel: Images L–P: GFP was expressed in a variety of cell types after LDL-mediated transfection with pEGFP-N1 plasmid DNA. Images are merged overlays of brightlight and fluorescence micrographs. L: MCF7, and M: CHO cells at 2 h after transfection. N: NIH/3T3 cells at 18 h after transfection. O, P: HeLa cells at 1 h (O) and 18 h (P) post transfection. GFP expression appears as pronounced green fluorescence.

immediately after collection of tissue sections on day 2 are shown in **Fig. 3**. In the top row, GFP fluorescence is seen in the basal cell layer of the stratified squamous epithelium of the esophagus (Fig. 3A). No fluorescence is visible in the lamina propria region located at the lower portion of the image. GPF fluorescence is also seen in the spinal cord (Fig. 3C), lung (Fig. 3E), liver (Fig. 3G), and heart (Fig. 3I) in animals given rat LDL/pEGFP-N1 plasmid cocktail. Fluorescence was not detected in samples from both large and small intestine, brain, and dorsal aorta (images not included). The intense fluorescence seen in the spiral and tubular structures in the lung image (Fig. 3E) and the endothelium of the hepatic vein (Fig. 3G) was a matter of concern, because these structures are characterized by elastic laminae, which are known to autofluoresce. However, images of tissues obtained from control animals treated only with the *Hin*dIII-cut pEGFP-N1 (Fig. 3B, esophagus; D, brain; F, lung; H, liver; J, heart) showed no or low intensity fluorescence. In the rat inoculated with human LDL/pEGFP-N1 complex, intense fluorescence is visible in the myocardial tissue (Fig. 3K). Results obtained from other tissues from this animal were inconclusive.

Separate experiments were conducted to compare tissue distribution of the luciferase gene delivered as pGL2-Control DNA alone or complexed to LDL, cationic liposome, or to a mixture of LDL and liposome. Each rat was given one injection of DNA/transfection agent mix at a single site (see Methods). DNA extracted from each tissue was analyzed by PCR using luciferase-specific primers (Fig. 3, lower panel). A qualitative comparison of these results is shown in **Table 4**. Briefly, pGL2-Control vector alone appears to transfect liver, brain, and spleen at barely detectable levels. Whether the DNA binds to LDL particles present in the rat's plasma was not determined in these studies. LDL-mediated delivery was highly effective in the kidney and spleen, somewhat effective in brain and heart, but negative results are seen in the lungs and liver. The difference between results obtained in LDL-mediated transfection with GFP gene and the luciferase gene, both driven by the CMV promoter, may be attributed to different inoculation methods (multiple sites of inoculation/application in the former study vs. single site injection in the latter experiment). The liposome-plasmid complex was highly effective in liver and visibly effective in heart, transfected lung, kidney, and spleen at lower levels, but was negative in brain. The LDL/Liposome mix was highly effective in delivery of the plasmid to the heart and lung, less effective in spleen, only slightly effective in brain, and negative in liver and kidney. These preliminary results confirm that LDL particles are useful transfection vectors in vivo.

Synthetic peptide studies

Synthetic peptides of apo B100 Regions 1 and 2, presented in Tables 1 and 3, were obtained to evaluate the role of apo B100 in nucleic acid-binding, transport, and delivery. Two additional criteria were important in selecting these regions: presence of an apo E receptor ligand analog sequence and solubility (hydrophilicity and hydrophobicity), based on ratio of charged and polar amino acids to nonpolar, hydrophobic amino acids (4). The N terminus, residues 0012 thru 0160 (Region 1), and the known B/E receptor ligand region, residues ^{3313}Asp thru Ser^{3458} (Region 2), meet these criteria.

In EMSA studies, synthetic peptides B1-1 (^{0014}Lys-Glu^{0054}) and B1-2 (^{0055}Leu-Ala^{0096}) were shown to bind phMGFP DNA in the presence of 10 mM $MgCl_2$ (**Fig. 4**). Electrophoresis was performed in a 0.8% agarose and TA buffer. Results are shown in image A: for plasmid only, lane 1; plasmid plus 3, 6, and 12 μg of each peptide, B1-1 (^{0014}Lys-Glu^{0054}), lanes 2, 3, and 4, respectively; B1-2 (^{0055}Leu-Ala^{0096}), lanes 5–7; B2-1 (^{3313}Asp-Glu^{3355}), lanes 8–10; B2-2 (^{3356}Gly-Thr^{3431}), lanes 11–13; B1-1/B1-2 (R1) mix, 8 μg each, lane 14; and B2-1/B2-2 (R2) mix, 8 μg each, lane 15. Peptides visualized with Coomassie Blue dye in the gel are in image B. Results for peptide B2-3 (^{3358}Thr-Leu^{3373}), the known B/E receptor ligand, mixed with plasmid are shown in image C, DNA alone (lane 16), and DNA plus 10 μg peptide (lane 17).

Cocktails of B1-1/B1-2, Region 1, mixed with phMGFP were shown to deliver BOBO-1-labeled DNA to preconditioned HeLa cells within 1 h after addition of peptides/DNA complex to the medium (**Fig. 5A–H**). As time progressed, fluorescent, amorphous cell debris was observed. Cell experiments using peptides alone confirmed the cytotoxicity of Region 1 peptides (Fig. 5I, J), as indicated by the accumulation of Trypan blue dye in the cell culture treated with these peptides.

Synthetic peptides B2-1 (^{3313}Asp-Glu^{3355}), B2-2 (^{3356}Gly-Thr^{3401}), and B2-3 (^{3358}Thr- Leu^{3373}) were also shown to bind phMGFP DNA in the presence of 10 mM $MgCl_2$ (Fig. 4). Binding of the B2-3 peptide appeared to be weak, resulting only in a smearing appearance of the plasmid band. Cocktails containing peptides B2-2 and B2-3 with DNA were ineffective in transfecting HeLa cells (results not included). Further, these peptides were shown to be noncytotoxic (Fig. 5K, L).

DISCUSSION

LDL and VLDL transport lipids in the plasma and are characterized by apo B100 as their major protein. We have demonstrated plasmid DNA-binding capacity for these lipoproteins and that DNA bound to LDL is transferred to the cell nucleus. Our results confirm that LDL is an effective transfection vector in vivo and in vitro. Lp (a), another apo B 100-containing particle that may be present in small quantities in the LDL fraction with buoyant density < 1.050 g/ml (48), was not shown to possess DNA-binding capacity (20). Apo (a), the massive, hydrophilic molecule covalently linked and noncovalently attached to apo B100 to form Lp (a), contains only one Arg/Lys-rich cluster in the kringle domain in the single copy of kringle type 11 and two in the putative serine protease domain (49, 50). Kringle types 1–10 in apo (a) are similar to plasminogen kringle 4 (49) and are devoid of basic amino acid clusters and motifs suggestive of nucleic acid binding or nuclear translocation. The noncovalent interactions between apo (a)

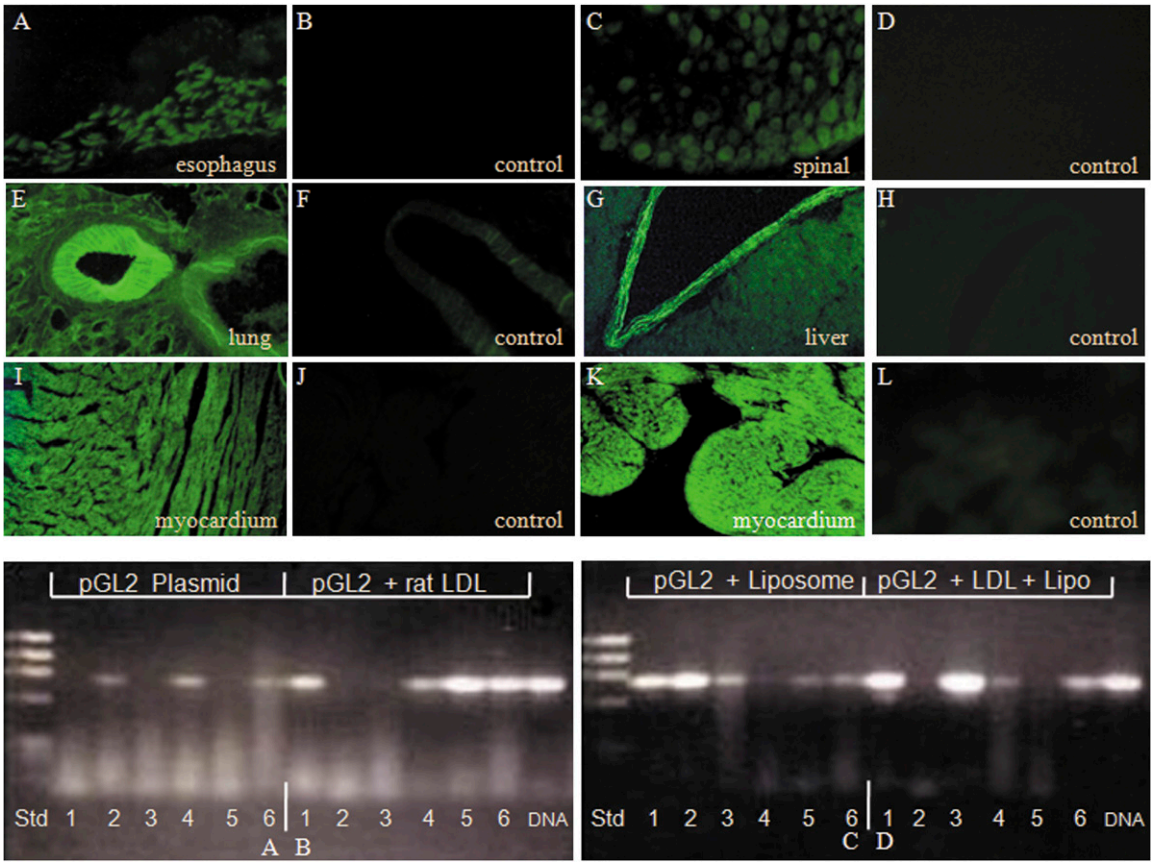

Fig. 3. GFP expression and tissue distribution in rat. Top panel: GFP was expressed in esophagus (A, basal cells of stratified squamous epithelium), spinal cord (C), lung (E), liver (G), and heart (I, rat LDL-mediated transfection, and K, human LDL-mediated transfection). Frozen sections (4–8 μm thick) were obtained 2 days after the animals were given a mixture of LDL and linearized pEGFP-N1 DNA (images A, E, I, C, G, K) via multiple ports as described in Methods. GFP expression is not seen in control animals given interrupted plasmid DNA alone (B, D, F, H, J, L). Bottom panel: Distribution of luciferase gene in rat tissues. Lanes 1–6 show luciferase-specific 800 bp band in heart, liver, lung, brain, kidney, and spleen, respectively. Rats were transfected using pGL2-Control plasmid alone, or cocktails of rat LDL/pGL2-Control, Liposome/pGL2-control, and rat LDL/Liposome/pGL2-Control plasmid. DNA was extracted from rat tissues on day 2 after transfection and assayed using PCR with luciferase-specific primers 5′agcaactgcataaggctatg and 3′gttggtactagcaacgcact.

and apo B100 that probably involve lysine residues on the apo B100 (50) may render nucleic acid binding regions inaccessible. Hence, the Lp (a) particle may not have a role in the transport and delivery of nucleic acids.

LDL transfection capacity is likely based on apo B100, which provides the particle with DNA binding and cell entry potential. Sequence similarities in apo B100, apo E, and known nucleic acid-binding domains of transcriptional regulators (*irf* proteins and capsid/core proteins of Flaviviruses) provide an explanation for the capacity of LDL to bind DNA and RNA (17–23). These sequence similarities and experimental results strongly suggest that the first 160 residue N-terminal region of apo B100 and LDL receptor ligand region of apo E have functions of nucleic acid bind-

TABLE 4. Post-transfection distribution of the reporter genes in rat tissues

Tissue	pGL2 Plasmid only	LDL/pGL2 Complex	Liposome/pGL2 complex	LDL/liposome/ pGL2 complex	LDL/pEGFP-N1 complex*
Heart	Negative	Positive	Positive	Highly positive	Highly positive
Liver	Slightly positive	Negative	Highly positive	Negative	Highly positive
Lung	Negative	Negative	Slightly positive	Highly positive	Highly positive
Brain	Slightly positive	Positive	Negative	Slightly positive	Negative
Kidney	Negative	Highly positive	Slightly positive	Negative	Not examined
Spleen	Slightly positive	Highly positive	Slightly positive	Positive	Not examined
Esophagus	Not assayed	Not assayed	Not assayed	Not assayed	Positive
Spinal Cord	Not assayed	Not assayed	Not assayed	Not assayed	Positive

Rats were transfected in vivo with pGL2-Control plasmid, alone (column 2) or complexed to LDL (column 3), liposome (column 4), or to LDL/liposome mix (column 5). Presence of luciferase gene was determined by PCR in heart, liver, lung, brain, kidney, and spleen tissues (column 1) of the rat on day 2 after transfection. GFP expression in tissues of the rat transfected with pEGFP-N1 plasmid/LDL mix (column 6) was determined on day 2 and was based on green fluorescence in frozen section of different tissues. The data are illustrated in Fig. 3. * Inoculant was administered at multiple sites.

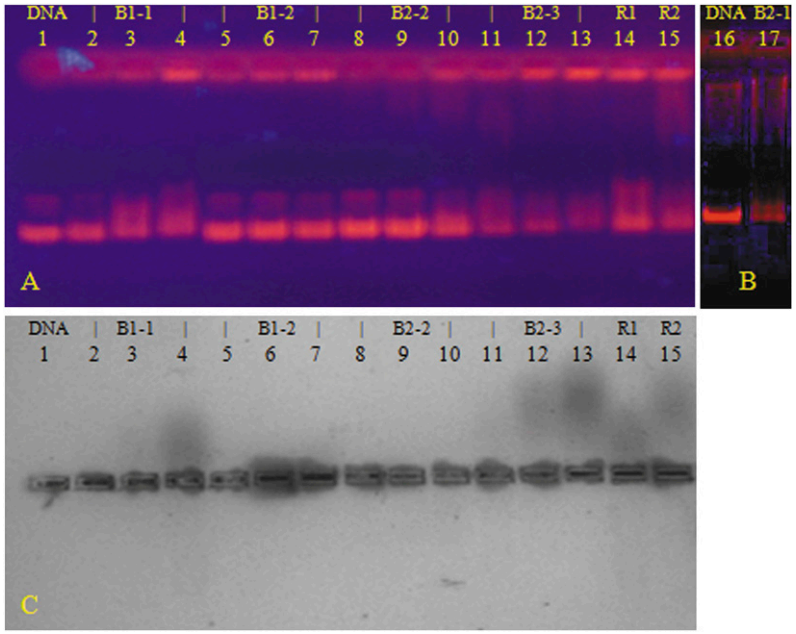

Fig. 4. EMSA of Apo B100-derived peptides and phMGFP. Sample cocktails were prepared using 0.42 μg of phMGFP plasmid and increasing quantities of each peptide derived from Region 1 (^{0014}Lys-Ala^{0096}) and Region 2 (^{3313}Asp-Thr^{3431}) of apo B100, as well as combinations of peptides derived from the same region. Amino acid sequences of the peptides are listed in Table 2 (Region 1) and Table 3 (Region 2). Electrophoresis was performed in a 0.8% agarose and TA buffer. A: lane 1: plasmid only; lanes 2, 3, and 4: plasmid plus 3, 6, and 12 μg, respectively, of peptide B1-1 (^{0014}Lys-Glu^{0054}); lanes 5, 6, and 7: plasmid plus 3, 6, and 12 μg, respectively, of peptide B1-2 (^{0055}Leu-Ala^{0096}); lanes 8, 9, and 10: plasmid plus 3, 6, and 12 μg, respectively, of the peptide B2-1 (^{3313}Asp-Glu^{3355}); lanes 11, 12, and 13: plasmid plus 3, 6, and 12 μg, respectively, of peptide B2-2 (^{3356}Gly-Thr^{3431}); lane 14: plasmid plus B1-1/B1-2 (R1) mix, 8 μg each; lane 15: plasmid plus B2-1/B2-2 (R2) mix, 8 μg each. B: pCMVTNT DNA, 1 μg alone (lane 16) and mixed with peptide B2-3 (^{3358}Thr-Leu^{3373}), 10 μg (lane 17). C: Same gel, lanes 1–15, stained with CBB.

ing. Synthetic peptides covering part of this apo B100 region, Region 1, bind plasmid DNA and substantiate this function to a degree, with the caveat that ligand specificity and peptide conformation are undetermined. Region 1 peptides also mediate cell entry for plasmid DNA, presumably via the B/E receptor and/or through the mechanism(s) used by Arg/Lys-rich cell-penetrating peptides (51). NLS sequence motifs are characterized by Arg/Lys-rich clusters, as in the DNA binding domains of most *irf* proteins and in the capsid/core proteins of *hcv* and other *Flaviviridae* viruses. Hence, apo B100 Region 1 contains motifs that impart nucleic acid binding, mediate cell uptake, and are apparently involved in transferring DNA into the cell nucleus.

Several studies suggest that *Flaviviridae* viruses may gain cell entry via the B/E receptor (24–26, 52). This mechanism is thought to involve the E1 and E2 structural proteins of the virus (26). Although one LRK motif occurs in envelope proteins of *dng1* and *dng3*, our examination of the primary structures of *dng1* envelope proteins did not reveal a complete apo E receptor ligand Arg/Lys-rich cluster similar to those contained in its capsid protein. However, four additional analogs of the **K/R**-XX-**K/R** are contained within the sequence spanning ^{0561}Gly to ^{0695}Leu of the *dng1* polyprotein sequence. In *hcv* and the four versions of *dng*, Arg/Lys-rich clusters containing multiple copies of the **K/R**-XX-**K/R** motif similar to those in the apo E receptor ligand sequence are located near the N termini of the capsid proteins. In *wnlv* and *ylfv*, the motifs are also located in the capsid proteins but are distal to the N terminus. It is therefore possible that cell entry is mediated by capsid proteins as well, and the almost ubiquitously expressed LDL B/E receptor may enhance viral infectivity and viability.

Flaviviral capsid proteins are multi-functional proteins, i.e., they bind nucleic acids, translocate nucleic acids to cell nucleus, have a role in dimerization of viral RNA, and regulate transcription (52–55). In the flaviviruses, once the polyprotein is expressed, the capsid proteins are cleaved by an endopeptidase at one of two dipeptide motifs of small hydrophobic amino acids such as Leu-Leu (26). Analogs of these dipeptide motifs are also present in a like-region of apo B100 as Ile-Ile and Leu-Leu. It is interesting to consider a similar mechanism is employed to release the N-terminal region of apo B100 for similar functions. Another property reported for the *wnlv* capsid/core protein is cytotoxicity (52, 56–58). This effect was also observed with the B1-1/B1-2 peptides mix on HeLa cells. One possible scenario would be that the N-terminal region of apo B100 is cleaved so that it may compete with viral capsid proteins for the nucleic acid and/or kill infected cells to suppress the infection process.

The synthetic peptides of the apo B100 region 2 were shown to bind DNA in EMSA. Region 2 sequence is similar to HSV5 UL122 helicase and *Flaviviridae* NS3 helicases and contains several analog motifs present in these viral proteins. Surprisingly, these peptides were ineffective in delivery of DNA to the cells despite the presence of the know B,E-receptor-binding ligand, possibly due to blocking of the receptor ligand site by DNA or inadequate conformation for docking with the receptor.

In summary, apo B100 and apo E, constituent proteins in LDL and VLDL, share many similarities with the flaviviral proteins that may be construed as analogs. Significant viral homologs were not found in the databases using recognized search algorithms and therefore lessen the possibility that these apolipoproteins are viral in origin. These apolipoproteins may have evolved as part of the immune system to address and/or eliminate viral (microbial) nucleic acids from circulation. Alternatively, we can consider also that flaviviruses may have evolved to mimic apo B100 and apo E domains to gain cell entry and evade the immune system of the host. Viral genomes are known to evolve faster than the

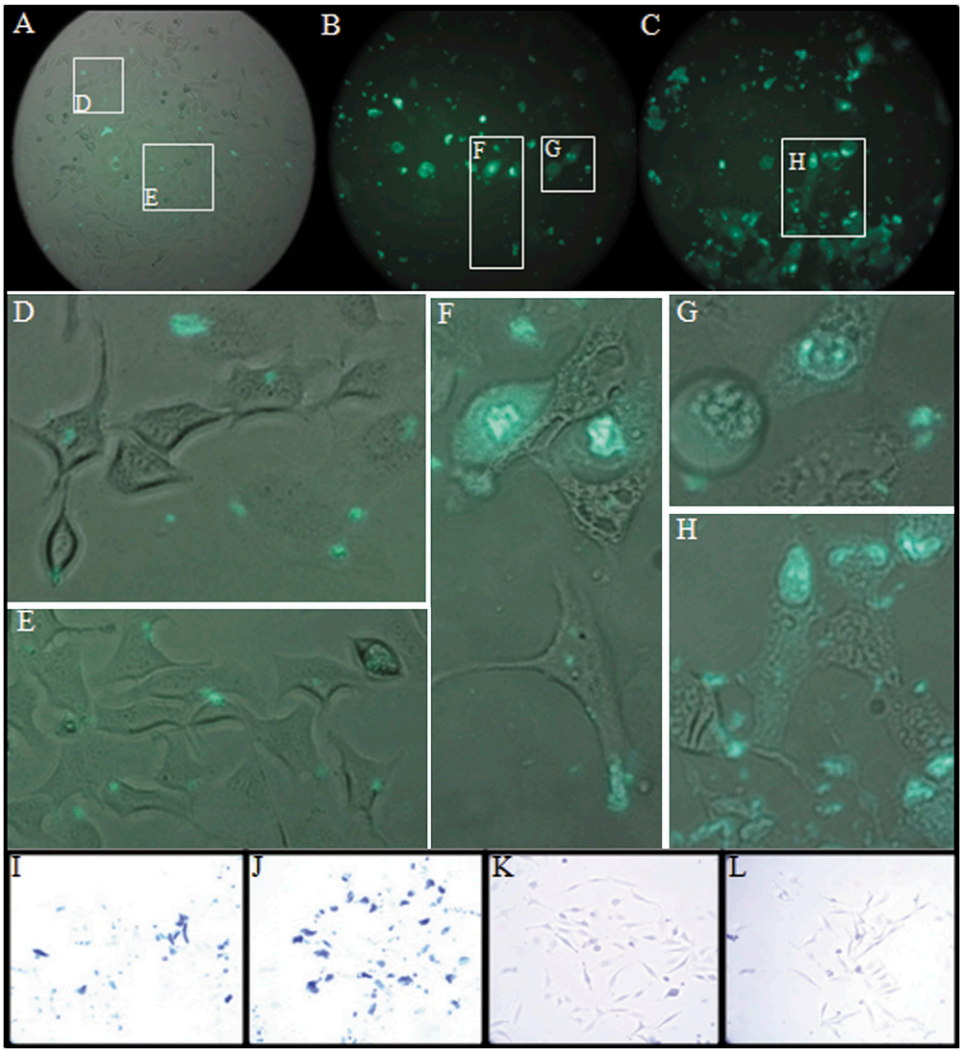

Fig. 5. Synthetic peptide mediated transfection of HeLa cells. Top panel: Synthetic peptide mediated transfection of HeLa cells with BOBO-1-labeled phMGFP plasmid. Dye-labeled plasmid DNA complexed to apo B100-derived peptides was used to transfect HeLa cells grown in DMEM medium as described in Methods. All frames show a merged overlay image of the fluorescence micrograph and the corresponding phase contrast version. Frames **A** thru **C** show cells transfected using cocktails of synthetic peptides B1-1 and B1-2 (Table 2) derived from N-terminal region of Apo B100 mixed with 1.0 μg BOBO-1-labeled phMGFP plasmid DNA: A: 1.5 nmol of B1-1 and 1.9 nmol of B1-2 plus plasmid; B: 5.9 nmol of B1-1 and 7.5 nmol of B1-2 plus labeled plasmid; C: 15 nmol of B1-1 and 19 nmol of B1-2 plus labeled plasmid. All transfection experiments were conducted in 400 μl of DMEM. Enlarged cut-out images in inserts D–H show intracellular loci of label. All images were obtained using a Zeiss Axiovert 25 scope and the Optronics MicroFire CCD camera. Bottom panel: Cytotoxic effects of peptides B1-1 and B1-2 on HeLa cells are demonstrated using Trypan Blue dye. Cytotoxicity caused by mixtures of synthetic peptides B1-1 and B1-2, 4 μg each peptide (frame I) and 10 μg each peptide (frame J), added to preconditioned HeLa cells in DMEM. In contrast, no cytotoxicity is seen for HeLa cells treated similarly with mixtures containing the same quantities of synthetic peptides B2-1/B2-2, frames K and L, respectively.

human genome. This ability paired with typically large population sizes can result in a fast selection of viral protein patterns that are able to mimic LDL receptor-binding motifs.

We surmise that the transport of nucleic acids by LDL may occur naturally and may be an essential function. Lipids may mediate the conformation state of the apo B100 for addressing a wide spectrum of nucleic acids as well as interactions with proteins. A function of apo B100- and apo E-containing particles may be in removing viral or other microbial nucleic acid debris from circulation. It is interesting to speculate that LDL may be also binding in vivo to circulating nucleic acids in plasma, which are present under normal conditions and are elevated in several diseases including acute inflammation and cancer (59–62). The role played by LDL and VLDL in the dissemination of *hcv* genomic RNA has been established by other investigators (16, 17, 19), and binding of LDL to genomic DNA was reported previously (18, 20, 23). Combined with the capacity of LDL to transfect different cell types and tissues, these observations suggest that perhaps LDL, and possibly VLDL, play a similar role in the mechanisms of metastatic disease.

These studies offer a new perspective in our understanding of the pathogenic nature of apo B100 lipoproteins. Changes in lipid content, chemical modifications of apo B100, accumulation of lipo-viral debris, and other changes affecting nucleic acid-binding capacity of LDL may alter functionality of these particles.

LDL and peptides derived from the apo B100 have great potential as nucleic acid transport and delivery vehicles with applications in gene replacement therapies, DNA vaccines, rapid creation of transgenic animals, and cell bioreactors in the production of pharmaceutical proteins. LDL and VLDL are the only delivery nanoparticles that can be used in autologous formulations. Unlike viral or synthetic vectors and cell penetrating peptides (63), autologous LDL will not elicit an immune response. LDLs are easily purified and can be readily stored for long periods in liquid nitrogen. These naturally occurring particles can be exploited in the development of accurate gene replacement formulations.

We thank Mario Diaz, Ph.D., UTB/TSC for his continued support. We also thank Ron Hoogeveen, Ph.D. and G. Andrew Bowden for their contributions in cell and animal studies. We especially thank Dr. Lawrence Chan for support and mentoring services provided under the SCORE pilot project.

REFERENCES

1. Davidsson, P., J. Hulthe, B. Fagerberg, B. M. Olsson, C. Hallberg, B. Dahllof, and G. Camejo. 2005. A proteomic study of the apolipoproteins in LDL subclasses in patients with the metabolic syndrome and type 2 diabetes. *J. Lipid Res.* **46:** 1999–2006.
2. Sacks, F. M., and H. Campos. 2003. Clinical review 163. Cardiovascular endocrinology 4. Low-density lipoprotein size and cardiovascular disease: a reappraisal. *J. Clin. Endocrinol. Metab.* **88:** 4525–4532.
3. Segrest, J. P., M. K. Jones, H. De Loof, and N. Dashti. 2001. Structure of apolipoprotein B-100 in low density lipoproteins. *J. Lipid Res.* **42:** 1346–1367.
4. Yang, C. Y., Z. W. Gu, S. A. Weng, T. W. Chen, H. J. Pownall, P. M. Sharp, S. W. Liu, W. H. Li, and A. M. Gotto, Jr. 1989. Structure of apolipoprotein B-100 of human low density lipoproteins. *Arteriosclerosis.* **9:** 96–108.
5. Chen, G. C., S. Zhu, D. A. Hardman, J. W. Schilling, K. Lau, and J. P. Kane. 1989. Structural domains of human apolipoprotein B-100. *J. Biol. Chem.* **264:** 14369–14375.
6. Chapman, M. J., P. M. Laplaud, G. Luc, P. Forgez, E. Bruckert, S. Goulinet, and G. LaGrange. 1988. Further resolution of the low density lipoprotein spectrum in normal human plasma: physicochemical characteristics of discrete subspecies separated by density gradient ultracentrifugation. *J. Lipid Res.* **29:** 442–458.
7. Voyno-Yasenetskaya, T. A., L. G. Dobbs, S. K. Erickson, and R. L. Hamilton. 1993. Low density lipoprotein- and high density lipoprotein-mediated signal transduction and exocytosis in alveolar type II cells. *Proc. Natl. Acad. Sci. USA.* **90:** 4256–4260.
8. Bochkov, V.N., V.A. Tkachuk, Y.S. Kuzmenko, Y.L. Borisova, F.R. Bühler, and T.J. Resink. 1994. Characteristics of low and high density lipoprotein binding and lipoprotein-induced signaling in quiescent human vascular smooth muscle cells. Mol Pharmacol. **45:** 262–270.
9. Cardin, A. D., T. L. Bowlin, and J. L. Krstenansky. 1988. Inhibition of lymphocyte proliferation by synthetic peptides homologous to human plasma apolipoproteins B and E. *Biochem. Biophys. Res. Commun.* **154:** 741–745.
10. Hui, D. Y., J. A. Harmony, T. L. Innerarity, and R. W. Mahley. 1980. Immunoregulatory plasma lipoproteins. Role of apoprotein E and apoprotein B. *J. Biol. Chem.* **255:** 11775–11781.
11. Kamanna, V. S., B. V. Bassa, and S. H. Ganji. 2008. Low density lipoprotein transactivates EGF receptor: role in mesanglial cell proliferation. *Life Sci.* **83:** 595–601.
12. Heo, K. S., D. U. Kim, L. Kim, M. Nam, S. T. Baek, S. K. Park, Y. Park, C. S. Myung, S. O. Hwang, and K. L. Hoe. 2008. Activation of PKC beta(II) and PKC theta is essential for LDL-induced cell proliferation of human aortic smooth muscle cells via Gi-mediated Erk 1/2 activation and Erg-1 upregulation. *Biochem. Biophys. Res. Commun.* **368:** 126–131.
13. Gonzalez-Timon, B., M. Gonzalez-Munoz, C. Zaragoza, S. Lamas, and E. M. Melian. 2004. Native and oxidized low density lipoprotein oppositely modulate the effects of insulin-like growth factor I on VSMC. *Cardiovasc. Res.* **61:** 247–255.
14. Ryoo, S. W., D. U. Kim, M. Won, K. S. Chung, Y. J. Jang, G. T. Oh, S. K. Park, P. J. Maeng, H. S. Yoo, and K. L. Hoe. 2004. Native LDL induces interleukin-8 expression via H202, p38 Kinase, and activator protein-1 in human aortic smooth muscle cells. *Cardiovasc. Res.* **62:** 185–193.
15. Pintus, G., B. Tadolini, A. M. Posadino, B. Sanna, M. Debidda, C. Carru, L. Deiana, and C. Ventura. 2003. PKC/Raf/MEK/ERK signaling pathway modulates native-LDL-induced E2F–1 gene expression and endothelial cell proliferation. *Cardiovasc. Res.* **59:** 934–944.
16. Nielsen, S. U., M. F. Bassendine, C. Martin, D. Lowther, P. J. Purcell, B. J. King, D. Neely, and G. L. Toms. 2008. Characterization of hepatitis C RNA-containing particles from human liver by density and size. *J. Gen. Virol.* **89:** 2507–2517.
17. Agaugue´, S., L. Perrin-Cocon, P. Andre, and V. Lotteau. 2007. Hepatitis C lipo-viro-particle from chronically infected patients interferes with TLR4 signaling in dendritic cell. *PLoS One.* **2:** e330 .
18. Guevara, J. G., Jr., R. C. Hoogeveen, and J. P. Moore. 2003. Lipoproteins as nucleic acid vectors. US Patent 6,635,623 B1.
19. Andre, P., F. Komurian-Pradel, S. Deforges, M. Perret, J. L. Berland, M. Sodoyer, S. Pol, C. Brechot, G. Paranhos-Baccala, and V. Lotteau. 2002. Characterization of low- and very-low-density hepatitis C virus RNA-containing particles. *J. Virol.* **76:** 6919–6928.
20. Guevara, Jr., J.G., Kang, Dc., and Moore, J.P. 1999. Nucleic acid-binding properties of low-density lipoproteins: LDL as a natural gene vector. *J. Protein Chem.* **18:** 845–857.
21. Sato, K., T. Takeshi, H. Okamoto, Y. Miyakawa, and M. Mayumi. 1996. Association of circulating Hepatitis G virus with lipoproteins for a lack of binding with antibodies. *Biochem. Biophys. Res. Commun.* **229:** 719–725.
22. Kabakov, A. E., V. A. Saenko, and A. M. Poverenny. 1991. LDL-mediated interaction of DNA and DNA-anti-DNA immune complexes with cell surface. *Clin. Exp. Immunol.* **83:** 359–363.
23. Steinman, C. R. 1984. Circulating DNA in systemic lupus erythematosus: isolation and characterization. *J. Clin. Invest.* **73:** 832–841.
24. Agnello, V., G. Abel, M. Elfahal, G. B. Knight, and Q-X. Zhang. 1999. Hepatitis C virus and other *Flaviviridae* viruses enter cells via low density lipoprotein receptor. *Proc. Natl. Acad. Sci. USA.* **96:** 12766–12771.
25. Burlone, M. E., and A. Budkowska. 2009. Hepatitis C virus cell entry: role of lipoproteins and cellular receptors. *J. Gen. Virol.* **90:** 1055–1070.
26. Lindenbach, B. D., H-J. Thiel, and C. M. Rice. 2007. *Flaviviridae*: the viruses and their replication. *In* Fields Virology. 5th edition. Knipe, D.M., and Howley, P.M., editors. Lippincott-Raven Publishers, Philadelphia. 1101–1152.
27. Zaiou, M., K. S. Arnold, Y. M. Newhouse, T. L. Innerarity, K. H. Weisgraber, M. L. Segall, M. C. Phillips, and S. Lund-Katz. 2000. Apolipoprotein E-low density lipoprotein receptor interaction: influences of basic residue and amphipathic α-helix organization in the ligand. *J. Lipid Res.* **41:** 1087–1095.
28. Lalazar, A., K. H. Weisgraber, S. C. Rall, Jr., H. Giladi, T. L. Innerarity, A. Z. Levanon, J. K. Boyles, B. Amit, M. Gorecki, R. W. Mahley, et al. 1988. Site-specific mutagenesis of human apolipoprotein E. *J. Biol. Chem.* **263:** 3542–3545.
29. Fujii, Y., T. Shimizu, M. Kusumoto, Y. Kyogoku, T. Taniguchi, and T. Hakoshima. 1999. Crystal structure of an *inf* -DNA complex reveals novel DNA recognition and cooperative binding to a tandem repeat of core sequences. *EMBO J.* **18:** 5028–5041.
30. Braddock, D. T., J. L. Baber, D. Levens, and G. M. Clore. 2002. Molecular basis of sequence-specific single-stranded DNA recognition by KH domains: solution structure of a complex between hnRNP K KH3 and single-stranded DNA. *EMBO J.* **21:** 3476–3485.

31. Grishin, N. V. 2001. KH domain: one motif, two folds. *Nucleic Acids Res.* **29:** 638–643.
32. Yang, C-Y., S-H. Chen, S. H. Gianturco, W. A. Bradley, J. T. Sparrow, M. Tanimura, W-H. Li, D. A. Sparrow, H. DeLoof, M. Rosseneu, et al. 1986. Sequence, structure, receptor-binding domains and internal repeats of human apolipoprotein B-100. *Nature.* **323:** 738–742.
33. Milne, R., R. Theolis, Jr., R. Maurice, R. J. Pease, P. K. Weech, E. Rassart, J. C. Fruchart, J. Scott, and Y. L. Marcel. 1989. The use of monoclonal antibodies to localize the low density lipoprotein receptor binding domain of apolipoprotein B*. *J. Biol. Chem.* **264:** 19754–19760.
34. Xu, T., A. Sampath, A. Chao, D. Wen, M. Nanao, P. Chene, S. G. Vasudevan, and J. Lescar. 2005. Structure of the dengue virus helicase/nucleoside triphosphatase catalytic domain at a resolution of 2.4 Å. *J. Virol.* **79:** 10278–10288.
35. Gorbalenya, A. E., and E. V. Koonin. 1988. One more conserved sequence motif in helicases. *Nucleic Acids Res.* **16:** 7734.
36. Schwartz, R., B. Helmich, and D. H. Spector. 1996. CREB and CREB-binding proteins play an important role in the IE2 86-kilodalton protein-mediated transactivation of the human cytomegalovirus 2.2-kilobase RNA promoter. *J. Virol.* **70:** 6955–6966.
37. O'Brien, K. D., K. L. Olin, C. E. Alpers, W. Chiu, M. Ferguson, K. Hudkins, T. N. Wight, and A. Chait. 1998. Comparison of apolipoprotein and proteoglycan deposits in human coronary atherosclerotic plaques – colocalization of biglycan with apolipoproteins. *Circulation.* **98:** 519–527.
38. Melnick, J. L., C. Hu, J. Burek, E. Adam, and M. E. DeBakey. 1994. Cytomegalovirus DNA in arterial walls of patients with atherosclerosis. *J. Med. Virol.* **42:** 170–174.
39. Wang, L., M. T. Walsh, and D. M. Small. 2006. Apolipoprotein B is conformationally flexible but anchored at a triolein/water interface: a possible model for lipoprotein surfaces. *Proc. Natl. Acad. Sci. USA.* **103:** 6871–6876.
40. Aitken, A. 1999. Review: protein consensus sequence motifs. *Mol. Biotechnol.* **12:** 241–253.
41. Jeong, E-J., G-S. Hwang, K. H. Kim, M. J. Kim, S. Kim, and K-S. Kim. 2000. Structural analysis of multifunctional peptide motifs in human bifunctional tRNA synthetase: identification of RNA-binding residues and functional implications for tandem repeats. *Biochemistry.* **39:** 15775–15782.
42. Massey, S. E. 2006. Basic faced α-helices are widespread in the peptide extensions of the eukaryotic aminoacyl-tRNA synthetases. *In Silico Biol.* **6:** 259–273.
43. Berry, D. M., P. Nash, S. K-W. Liu, T. Pawson, and C. J. McGlade. 2002. A high-affinity Arg-X-X-Lys SH3 binding motif confers specificity for the interaction between Gads and SLP-76 in T cell signaling. *Curr. Biol.* **12:** 1336–1341.
44. Lau, J. F., J-P. Parisien, and C. M. Horvath. 2000. Interferon regulatory factor subcellular localization is determined by a bipartite nuclear localization signal in the DNA-binding domain and interaction with cytoplasmic retention factors. *Proc. Natl. Acad. Sci. USA.* **97:** 7278–7283.
45. Escalante, C. R., J. Yie, D. Thanos, and A. K. Aggarwal. 1998. Structure of IRF-1 with bound DNA reveals determinants of interferon regulation. *Nature.* **391:** 103-106.
46. Mastrangelo, E., M. Milani, M. Bollati, B. Selisko, F. Peyrane, V. Pandini, G. Sorrentino, B. Canard, P. V. Konarev, D. I. Svergun, et al. 2007. Crystal structure and activity of kunjin virus NS3 helicase; protease and helicase domain assembly in the full length NS3 protein. *J. Mol. Biol.* **372:** 444–455.
47. Walker, J. E., M. Saraste, M. J. Runswick, and N. J. Gay. 1982. Distantly related sequences in the alpha- and beta-subunits of ATP synthase, myosin, kinases, and other ATP-requiring enzymes and a common nucleotide binding fold. *EMBO J.* **1:** 945–951.
48. Reblin, T., D. Rader, U. Beisiegel, H. Greten, and H. B. Brewer, Jr. 1992. Correlation of apolipoprotein(a) isoproteins with Lp(a) density and distribution in fasting plasma. *Atherosclerosis.* **94:** 223–232.
49. McLean, J. W., J. E. Tomlinson, W. J. Kuang, D. L. Eaton, E. Y. Chen, G. M. Fless, A. M. Scanu, and R. M. Lawn. 1987. cDNA sequence of human apolipoprotein(a) is homologous to plasminogen. *Nature.* **330:** 132–137.
50. Weisel, J. W., C. Nagaswami, J. L. Woodhead, A. A-R. Higazi, W. J. Cain, S. M. Marcovina, M. L. Koschinsky, D. B. Cines, and K. Bdeir. 2001. The structure of lipoprotein (a) and ligand-induced conformational changes. *Biochemistry.* **40:** 10424–10435.
51. Melikov, K., and L. V. Chernomordik. 2005. Arginine-rich cell penetrating peptides: from endosomal uptake to nuclear delivery. [Review] *Cell. Mol. Life Sci.* **62:** 2739–2749.
52. Weiner, D. B., and J-S. Yang. 2002. Compositions and methods of using capsid protein from Flaviviruses and Pestiviruses. US Patent Application 20020164349.
53. Sangiambut, S., P. Keelapang, J. Aaskov, C. Puttikhunt, W. Kasinrerk, P. Malasit, and N. Sittisombut. 2008. Multiple regions in dengue virus capsid protein contribute to nuclear localization during virus infection. *J. Gen. Virol.* **89:** 1254–1264.
54. Cristofari, G., R. Ivanyi-Nagy, C. Gabus, S. Boulant, J-P. Lavergne, F. Penin, and J-L. Darlix. 2004. The hepatitis C virus core protein is a potent nucleic acid chaperone that directs dimerization of the viral (+) strand RNA *in vitro*. *Nucleic Acids Res.* **32:** 2623–2631.
55. Wang, S-H., W-J. Syu, K-J. Huang, H-Y. Lei, C.-W. Yao, C.-C. King, and S.-T. Hu. 2002. Intracellular localization and determination of a nuclear localization signal of the core protein of dengue virus. *J. Gen. Virol.* **83:** 3093–3102.
56. Chu, J. J., and M. L. Ng. 2003. The mechanism of cell death during West Nile virus infection is dependent on initial infectious dose. *J. Gen. Virol.* **84:** 3305–3314.
57. Mori, Y., T. Okabayashi, T. Yamashita, Z. Zhao, T. Wakita, K. Yasui, F. Hasebe, M. Tadano, E. Konishi, K. Moriishi, et al. 2005. Nuclear localization of Japanese encephalitis virus core protein enhances viral replication. *J. Virol.* **79:** 3448–3458.
58. Shimoike, T., S. Mimori, H. Tani, Y. Matsuura, and T. Miyamura. 1999. Interaction of hepatitis C virus core protein with viral sense RNA and suppression of its translation. *J. Virol.* **73:** 9718–9725.
59. Suzuki, N., A. Kamataki, J. Yamaki, and Y. Homma. 2008. Characterization of circulating DNA in healthy human plasma. *Clin. Chim. Acta.* **387:** 55–58.
60. Fleischhacker, M., and B. Schmidt. 2007. Circulating nucleic acids (CNAs) and cancer: a survey. Review. *Biochim. Biophys. Acta.* **1775:** 181–232.
61. Goebel, G., M. Zitt, M. Zitt, and H. M. Muller. 2005. Circulating nucleic acids in plasma or serum (CNAPS) as prognostic and predictive markers in patients with solid neoplasias. *Dis. Markers.* **21:** 105–120.
62. Jahr, S., H. Hentze, S. Englisch, D. Hardt, F. O. Fackelmayer, R-D. Hesch, and R. Knippers. 2001. DNA fragments in the blood plasma of cancer patients: quantitations and evidence for their origin from apoptotic and necrotic cells. *Cancer Res.* **61:** 1659–1665.
63. Herce, H. D., and A. E. Garcia. 2007. Review: cell penetrating peptides: how do they do it? *J. Biol. Phys.* **33:** 345–356.